International Telecommunication Union

ITU-R

Radiocommunication Sector of ITU

Report ITU-R RS.2456-0
(06/2019)

Space weather sensor systems using radio spectrum

RS Series
Remote sensing systems

International Telecommunication Union

Foreword

The role of the Radiocommunication Sector is to ensure the rational, equitable, efficient and economical use of the radio-frequency spectrum by all radiocommunication services, including satellite services, and carry out studies without limit of frequency range on the basis of which Recommendations are adopted.

The regulatory and policy functions of the Radiocommunication Sector are performed by World and Regional Radiocommunication Conferences and Radiocommunication Assemblies supported by Study Groups.

Policy on Intellectual Property Right (IPR)

ITU-R policy on IPR is described in the Common Patent Policy for ITU-T/ITU-R/ISO/IEC referenced in Resolution ITU-R 1. Forms to be used for the submission of patent statements and licensing declarations by patent holders are available from http://www.itu.int/ITU-R/go/patents/en where the Guidelines for Implementation of the Common Patent Policy for ITU-T/ITU-R/ISO/IEC and the ITU-R patent information database can also be found.

Series of ITU-R Reports

(Also available online at http://www.itu.int/publ/R-REP/en)

Series	Title
BO	Satellite delivery
BR	Recording for production, archival and play-out; film for television
BS	Broadcasting service (sound)
BT	Broadcasting service (television)
F	Fixed service
M	Mobile, radiodetermination, amateur and related satellite services
P	Radiowave propagation
RA	Radio astronomy
RS	**Remote sensing systems**
S	Fixed-satellite service
SA	Space applications and meteorology
SF	Frequency sharing and coordination between fixed-satellite and fixed service systems
SM	Spectrum management

Note*: This ITU-R Report was approved in English by the Study Group under the procedure detailed in Resolution ITU-R 1.*

Electronic Publication
Geneva, 2019

REPORT ITU-R RS.2456-0

Space weather sensor systems using radio spectrum

(2019)

Scope

This Report provides a summary of space weather sensor systems using radio spectrum which are used for detection of solar activity and the impact of solar activity on the Earth, its atmosphere and its geospace. Annex 1 to the Report provides a categorization of selected RF-based sensors with regard to their support of current space weather products.

Keywords

Space weather, Earth exploration-satellite service (passive) systems, radio astronomy, radar, radiolocation

Abbreviations/Glossary

AARDDVARK	Antarctic-Arctic Radiation-belt (Dynamic) Deposition – VLF Atmospheric Research Konsortium
AEU	Antenna Element Unit
AGW	Atmospheric Gravity Waves
AIS INGV	Advanced Ionospheric Sounder – Istituto Nazionale di Geofisica e Vulcanologia
AMISR	Advanced Modular Incoherent Scatter Radar
ARCAS	Augmented Resolution CALLISTO Spectrometer
ARTEMIS	Acceleration, Reconnection, Turbulence and Electrodynamics of the Moon's Interaction with the Sun
CALLISTO	Compound Astronomical Low-cost Low-frequency Instrument for Spectroscopy in Transportable Observatory
CMA	China Meteorological Administration
CME	Coronal Mass Ejection
COSMIC	Constellation Observing System for Meteorology, Ionosphere & Climate
CPU	Central Processing Unit
CW	Continuous Wave
DRAO	Dominion Radio Astronomy Observatory
EDP	Electron Density Profile
EISCAT	European Incoherent SCATter Scientific Association
eSWua	electronic Space Weather upper atmosphere
EUV	Extreme Ultraviolet
FFT	Fast Fourier Transform
FPGA	Field-Programmable Gate Array
GEO	Geostationary Earth Orbit

GIRO	Global Ionosphere Radio Observatory
GISTM	GNSS Ionospheric Scintillation and TEC Monitor
GLONASS	Globalnaya Navigazionnaya Sputnikovaya Sistema, or Global Navigation Satellite System
GloRiA	Global Riometer Array
GNSS	Global Navigation Satellite System
GNSS-RO	Global Navigation Satellite System Radio-occultation
GPS	Global Positioning System
HF	High Frequency
HFDF	HF Direction Finding
HSRS	Humain Solar Radio Spectrometer
IMF	Interplanetary Magnetic Field
IPS	Interplanetary Scintillation
ISR	Incoherent Scatter Radar
KSWC	Korean Space Weather Center
LEO	Low-Earth Orbit
LOFAR	LOw Frequency Array
LPDA	Log Periodic Dipole Array
LWA	Long Wavelength Array
MAARSY	Middle Atmosphere Alomar Radar System
METAIDS	Meteorological Aids
MEO	Medium Earth Orbit
MEXART	Mexican Array Radio Telescope
MF	Medium Frequency
MHGF	Millstone Hill Geospace Facility
MIT	Massachusetts Institute of Technology
MLT	Mesosphere/lower thermosphere
MMS	Magnetospheric Multiscale (MMS) mission
MR	Meteor Radar
NDA	Nançay Decameter Array
NENUFAR	New Extension in Nançay Upgrading LOFAR
NoRP	Nobeyama Radio Polarimeter
NRH	Nançay Radioheliograph
ORFEES	Observation Radio Fréquences pour l’Etude des Eruptions Solaires
PBL	Plasmasphere Boundary Layer

PCAs	Polar Cap Absorption events
PFISR	Poker Flat Incoherent Scatter Radar
Pi2 pulsations	Irregular, damped ULF range magnetic pulsations occurring in connection with magnetospheric substorms.
Plasma Frequency	The natural frequency of a plasma oscillation, $f_p = 8920\sqrt{n_e}$ Hz, where n_e is the electron density per cubic centimetre
PNT	Positioning, Navigation and Timing
PSD	Power Spectral Density
QDC	Quiet-Day Curve
RO	Radio Occultation
Riometer	Relative Ionospheric Opacity Meter for Extra-Terrestrial Emissions of Radio noise
RIMS	Radio Interference Monitoring Systems
RISR	Resolute Bay Incoherent Scatter Radar
RNSS	Radionavigation satellite service
RSTN	Radio Solar Telescope Network
SATCOM	Satellite Communications
SEP	Solar Energetic Particles
SEON	Solar Electro-Optical Network
SFU	Solar Flux Unit; One SFU = 10^{-22} watt per square meter-hertz, or 10 000 Jansky
SIDC	Solar Influences Data Analysis Center
SKiYMET	All-Sky Interferometric Meteor Radar
SRS	Solar Radio Spectrograph
STEC	Slant Total Electron Content
SuperDARN	Super Dual Auroral Radar Network
TEC	Total electron content
TSI	Total solar irradiance
TID	Travelling ionospheric disturbance
ULF	Ultra low frequency
URSI	International Union of Radio Science
VLF	Very low frequency
WMO	World Meteorological Organization

Related ITU Recommendations/Reports

Report ITU-R RS.2178 – The essential role and global importance of radio spectrum use for Earth observations and for related applications (see Part B, section B.1.2).

TABLE OF CONTENTS

1 Introduction

Space weather refers to the physical processes occurring in the space environment that ultimately affects human activities on Earth and in space. Space weather is influenced by the solar wind and the interplanetary magnetic field (IMF) carried by the solar wind plasma. A variety of physical phenomena are associated with space weather, including geomagnetic storms and substorms, energization of the Van Allen radiation belts, auroras, ionospheric disturbances and scintillation of satellite-to-ground radio signals and long-range radar signals, and geomagnetically induced currents at Earth's surface. Coronal mass ejections and their associated shock waves are also important drivers of space weather as they can distort the magnetosphere and trigger geomagnetic storms. Solar energetic particles (SEP), accelerated by coronal mass ejections or solar flares, are also an important driver of space weather.

FIGURE 1

Space Weather Phenomena

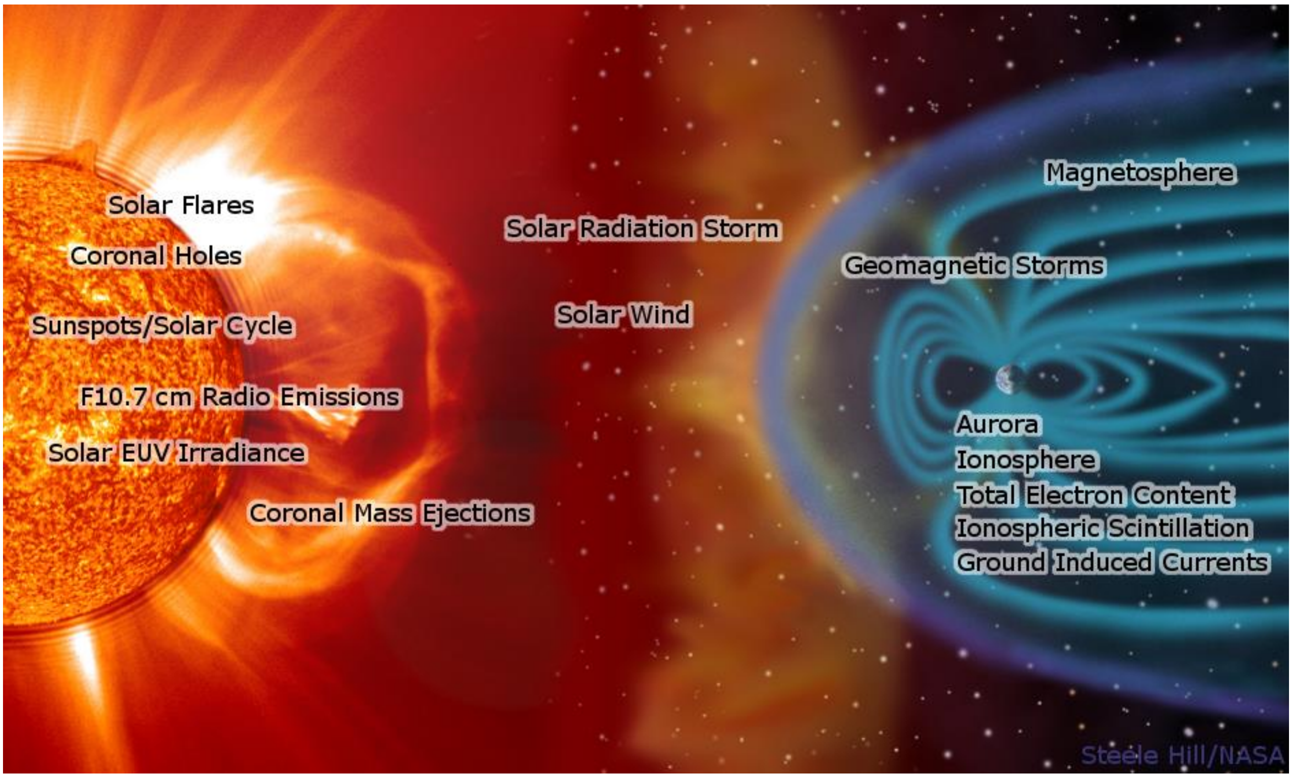

The electromagnetic radiation, traveling at the speed of light, takes about 8 minutes to move from Sun to Earth, whereas the energetic charged particles travel more slowly, taking from tens of minutes to hours to move from Sun to Earth. At typical speeds, the background solar wind plasma reaches Earth in about four days, while the fastest coronal mass ejections can arrive in less than one day. The solar wind interacts with the Earth's magnetic field and outer atmosphere in complex ways, causing strongly variable energetic particles and electric currents in the Earth's magnetosphere, ionosphere and surface. These disturbances can result in a hazardous radiation environment for satellites and humans at high altitudes, ionospheric disturbances, geomagnetic field variations, and the aurora. These effects can in turn impact a number of services and infrastructure located on the Earth's surface, airborne, or in Earth orbit. Disturbances in the ionosphere and atmosphere have important impacts on radio communication, satellitenavigation systems and heat the atmosphere which increases the atmospheric drag experienced by LEO satellites, including the International Space Station. Radionavigation-satellite service (RNSS) signals, which are used for a growing number of precision positioning, navigation, and timing applications, as well as for sounding the atmosphere using radio-occultation, are affected by signal propagation through the ionosphere. Strong spatial irregularities in the ionosphere (ionospheric scintillations) can cause loss of lock between a RNSS receiver and the satellite signals and can result in a total disruption of service. Variability in the total electron content (TEC) between the receiver and the satellite degrades RNSS positioning accuracy. Voltages induced into the electric power grid by the varying geomagnetic field can cause power outages affecting large geographic areas. Society is increasingly reliant on advanced – and interdependent – technology and its vulnerability to space weather hazards is also increasing. Space weather typically impacts infrastructure and services. The degradation or disruption of critical services in times of emergencies could also directly affect the health and welfare of individuals.

Space weather observations are needed:

1) to monitor and forecast the occurrence and probability of space weather disturbances (including monitoring those aspects of solar activity pertinent to space weather disturbances);

2) to drive hazard alerts when disturbance thresholds are crossed;

3) to maintain awareness of current environmental conditions;

4) to guide the design of both space-based systems (i.e. satellites and astronaut safety procedures) and ground-based systems (i.e. electric power grid protection and air traffic management);

5) to provide input data to develop and validate numerical models of space weather conditions; and

6) to conduct research that will enhance our understanding of the Sun and solar activity on Earth's extended atmosphere.

Forecasting space environment conditions is accomplished by monitoring the background solar magnetic configuration and precursors, such as flares, of phenomenon that occur on the Sun and which then propagate through the interplanetary medium before reaching Earth. Forecasts are primarily based on the measurement of the solar electromagnetic output in order to detect eruptive or pre-eruptive structures on the solar disc. Such forecasts require measurements in radio, visible, UV and X-ray wavelengths. Ideally, these observations should be obtained from different vantage points in the solar system to allow for three-dimensional stereo imaging of the Sun to obtain coronal magnetic structure using triangulation techniques.

When coronal mass ejections (CMEs) occur on the Sun, their initial velocity and size are measured to initiate models that predict their trajectories and arrival times at Earth. In addition, measurements are made of the plasma density, speed and magnetic field in the solar wind upstream from Earth to provide warnings of impending hazardous conditions. Monitoring CMEs can provide warnings of energetic particle radiation that can reach levels several orders of magnitude above the typical background levels and can persist for hours to days in length.

When the CME disturbances reach the outer boundary of Earth's magnetic field, the Earth's magnetic field is distorted. This distortion induces electrical currents through the magnetosphere, ionosphere and atmosphere and modifies the plasma and energetic particle distributions within the magnetosphere, including both the inner and outer radiation belts. Observations of the ionosphere/magnetosphere system from the ground and space are used in determining the current state of the near-Earth space weather environment and forecasting of the consequences of disturbances. Consequences may include disturbances to electric power grids, disruption to communications, damage to on-orbit satellites, and an increase in the hazardous radiation environment for humans at high altitudes (in space and on commercial aircraft flights near the Earth's poles) with a consequential impact on aviation operations.

Figure 2 presents a summary of the radio disturbances caused by a single solar flare. It represents a typical sequence of events stretching from fractions of a minute to days after the solar eruption.

FIGURE 2

Typical sequence of events following a solar flare

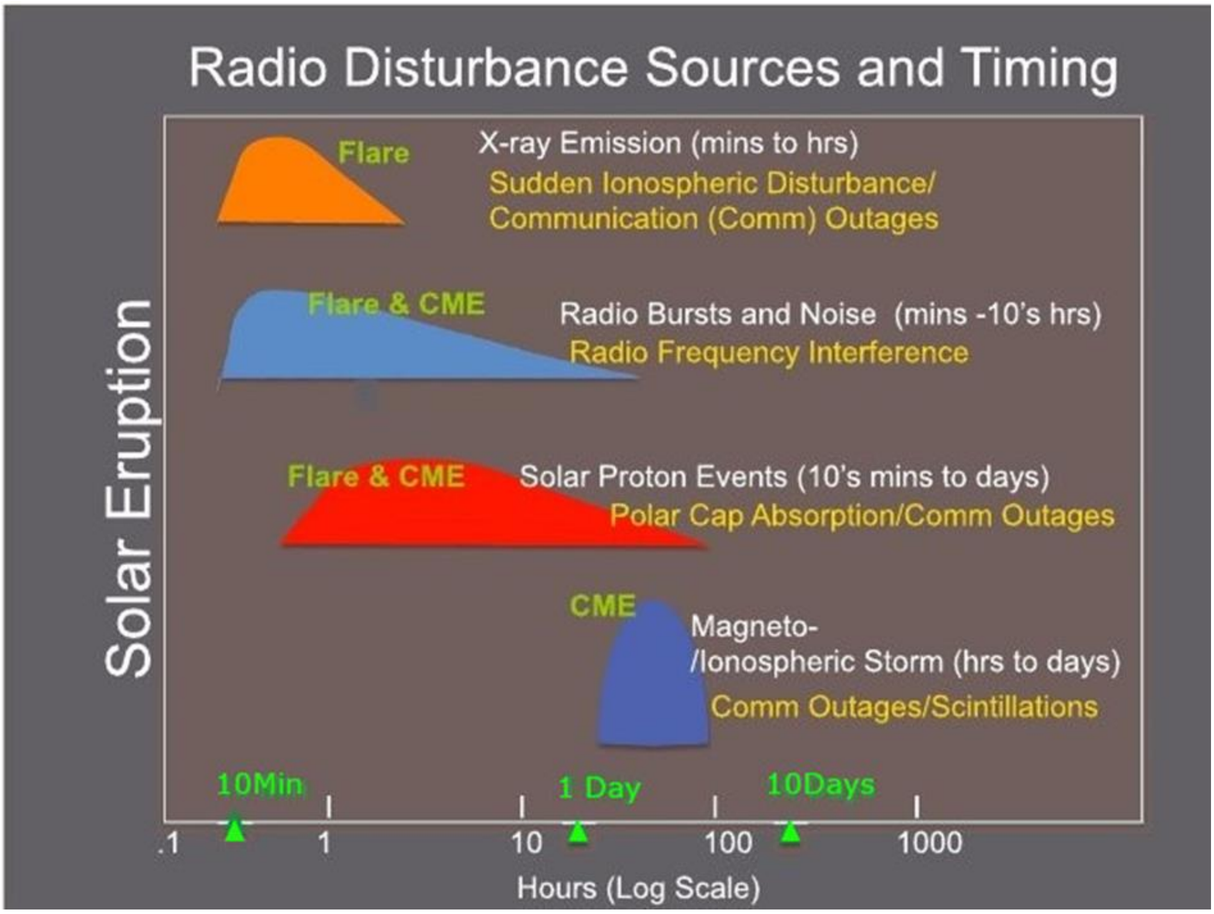

A comprehensive space weather observation network must include both ground-based and space-borne observatories as some environments to be measured are inaccessible to space-based sensors. The total range of necessary space weather measurements are obtained by both active and passive sensing techniques which are space-based and ground-based.

The Carrington event of 1859 was a space weather event of such intensity that it interrupted terrestrial telegraph services. Telegraph systems all over Europe and North America failed, and in some cases telegraph pylons threw sparks and telegraph operators received electric shocks. Should such a space weather event reoccur it is anticipated that space-based assets will be damaged if not destroyed. According to a 2009 report from the U.S. National Academy of Sciences, "The socioeconomic impacts of a long-term outage, such as one requiring replacement of permanently damaged transformers, could be extensive and serious. According to an estimate by the Metatech Corporation, the total cost of a long-term, wide-area blackout caused by an extreme space weather event could be as much as \$1 trillion to \$2 trillion during the first year, with full recovery requiring 4 to 10 years depending on the extent of the damage". After such an event, only terrestrial-based solar monitors would remain available for providing warnings of subsequent space weather events. The only all-weather systems available for crucial space weather monitoring are systems using radio-frequencies. Therefore, because redundancy cannot be assured, it is critical that all space based and terrestrial solar radio monitors receive appropriate levels of protection in the Radio Regulations.

1.1 Radio frequency observations

Solar

Radio flux observations in different frequencies are used to monitor the time evolution and classifications of the most short-lived solar features such as solar radio bursts. Dynamic radio spectra are used to further characterize flares, CMEs and the associated shock waves through the associated types II, III, IV radio emission signatures (see Table 2). Solar flux at 10.7 cm wavelength (2800 MHz) is also recorded daily and used for long-term solar variability and climatological studies and as a proxy for other solar parameters used in models of the Earth's atmosphere. In addition, the Total Solar Irradiance (TSI) measurements, widely utilized in atmospheric applications, can also be used to track the short-term and long- term variations of the Sun as a part of space weather research.

Solar electromagnetic radiation measurements in the radio domain at selected frequencies are useful in confirming the solar origin of failure or degradation in societal applications.

Space weather forecasts, triggered by the occurrence of radio bursts, as well as the speed of shocks in the corona and solar wind, require the observation of dynamic radio spectra between 20 MHz and 2 GHz with a cadence of 1 to 60 seconds and a delay of availability of 1 and 5 minutes. Such measurements are obtained by ground-based infrastructure which require contributions from observatories around the globe to achieve 24 hour coverage.

Ionosphere

The ionosphere is the electrically ionised part of the upper atmosphere (50-1 000 km) embedded in the electrically neutral 'thermosphere' with its upper boundary coupled to magnetosphere and lower boundary coupled to atmosphere. The properties of ionosphere are controlled by fluctuations in high-energy solar radiation (EUV and X-rays), by energetic particle fluxes through their interaction with the solar wind and the Earth's magnetosphere and by dynamic processes in the thermosphere and the lower atmosphere. The ionosphere varies appreciably from day to day, hour to hour, and minute to minute and is characterised by phenomena having very different characteristics at high and low latitudes in comparison to mid-latitudes.

The most important ionospheric variable is the electron density whose changes in time and space affect several types of infrastructure on Earth and in space. Its altitude variations, together with some other parameters, define the traditional division of the ionosphere into D, E, and F layers, started from the lowest. However, the ionospheric electron density is rarely measured in-situ. Instead, ionospheric monitoring techniques commonly utilize radio waves whose propagation variables (i.e. amplitude, phase, travel time and polarization) are affected by the ionospheric plasma.

The variability of the ionosphere impacts the performance of RNSS, communication systems relying on HF (3-30 MHz) radio wave propagation, satellite systems using radio signals, and, to a lesser degree, remote sensing applications such as Synthetic Aperture Radars.

The ionospheric effect on RNSS signals both from the ground and space can manifest itself as:

1) impacts on the multi-frequency differential signal delay on the RNSS signal. This is proportional to the Total Electron Content (TEC), which is the integral of the electron density along the radio link path. TEC may be geometrically specified as slant TEC (STEC) along the radio link or as vertically integrated electron density (VTEC). TEC observations

are required by Positioning, Navigation and Timing (PNT) applications using single frequency RNSS receivers. Observations of STEC are required to drive alerts for spatio-temporal ionospheric gradients, which can impact PNT applications relying on network based corrections, such as network real time kinematic;

2) scintillations (rapid fluctuations in amplitude and/or phase) of the RNSS signal caused by ionospheric distortions. The scintillation intensity indices (amplitude S4 and phase $\sigma\phi$,) are the effective indicators for describing the degree of ionospheric perturbation due to small scale irregularities and plasma bubbles. These perturbations can cause fluctuations in the amplitude and phase of Global Navigation Satellite Systems (GNSS) signals and lead to severe degradation in the quality of related applications. Scintillation observations for RNSS and satellite communication (SATCOM) signals passing through the ionosphere at a particular location are used to provide warnings of potential degradations of PNT accuracy and SATCOM conditions.

Active sounding of the ionosphere using HF radio waves with ionosondes is conducted in both vertical incidence and oblique transmission modes. Ionosondes provide a set of E- and F- region ionospheric state variables, which are important for characterising GNSS and HF impacts, such as:

1) foF2 – The variable foF2 is the maximum radio frequency reflected vertically from the ionospheric F-region. foF2 observations are used to derive the maximum useable frequency for specific HF radio broadcast ranges or point to point connections.

2) hmF2 – hmF2 is the height of the density peak of the F2 layer. hmF2 observations are critical for HF Direction Finding (HFDF) and radar operations.

3) spread-F – Spread-F is the amount of range spread of the HF radiowave reflected from the F region. The spread-F is used to classify conditions for HF radio communications and HFDF.

4) foEs – the variable foEs represents the electron density of a thin but dense sporadic E layer near 110 km, and the increase of Es causes extraordinary propagation of both HF and VHF (30-300 MHz) radio waves.

Observations of Ionospheric radio absorption in the D-region are also important for characterizing the impacts on communications. These include:

1) Polar Cap Absorption events (PCAs) which occur in polar areas when solar energetic particles ionize the ionospheric D-region and result in the complete absorption of incident HF radio waves. PCAs may last for several days.

2) HF Blackouts occur when large solar X-ray flares cause considerable D-region ionization on the sunlit side of the Earth. This absorption may last several hours and is observed using ground-based passive monitoring of the background Cosmic Radio Noise with riometers (Relative Ionospheric Opacity METERs).

The ionosonde observations and Very Low Frequency (VLF) (3-30 kHz) measurements also help evaluate signal absorption in the D-region.

2 Space weather sensor systems using radio spectrum

Operational space weather products and services are delivered by a network of about 20 organizations around the globe. The products and services which support space weather needs are organized in four broad categories: Ionospheric, Geomagnetic, Energetic Particles, and Solar and Interplanetary (solar wind). Currently, space weather observational products are being made available under these categories at the World Meteorological Organization (WMO) Space Weather Product Portal (http://www.wmo.int/pages/prog/sat/spaceweather-productportal_en.php). A larger number of products are distributed by the international space environment centres that have not been included in the Portal. This report focuses on space weather sensor systems using radio spectrum.

2.1 Ionospheric observations

There are eight active and passive RF-based sensor techniques used in monitoring the ionosphere.

2.1.1 Radionavigation-satellite service (RNSS) receiver

TEC along a given propagation path can be measured by tracking the time delay and phase shift of radio signals of a RNSS satellite by a space-borne or ground-based receiver. As the satellites move relative to the receiver, the TEC along the many available propagation paths is used to determine the distribution of ionospheric electron density.

An RNSS receiver used for space weather measures amplitude, pseudorange, and phase measurements at two or more radio frequencies. The dispersive nature of the Earth's ionosphere causes the signal paths for each frequency to be slightly different. There are several methods for extracting the ionospheric delay along the RNSS receiver signal path. Selection of a specific method depends on the desired geophysical retrieval product, data noise, desired retrieval accuracy and spatial resolution.

Ground-based RNSS receivers are numerous and widely used for space weather, meteorological and many other applications. These systems provide accurate information about the horizontal electron density gradients, but limited information about the vertical gradients. Ionospheric scintillation is typically measured by application of this method at an enhanced sampling rate (typically 100 Hz). RNSS System 1A (Table 4) is one example of a RNSS system configured for scintillation measurements.

On the other hand, radio occultation (RO) data obtained from low-Earth orbit (LEO) satellites equipped with RNSS receivers contain high-resolution information about the vertical gradients and limited information about the horizontal gradients. Thus, the RO data augment the ground-based RNSS measurement coverage on a planetary scale and, being based on limb sounder measurements, provide vertical distribution information. The global coverage of the space-based constellation is particularly important over ocean areas where a ground-based RNSS network is impractical. Measurements from space-based RNSS-RO receivers provide one of the only ways of obtaining global vertical profiles of electron density.

The geometry of RO measurements is shown in Fig. 3. During a RNSS occultation the receiver in low Earth orbit receives the transmitted signal from the RNSS satellite through the Earth's limb. The RNSS receiver observes changes in delay of the signal that are related to slowing and bending of the signal path.

FIGURE 3

Geometry of RNSS radio occultation measurements

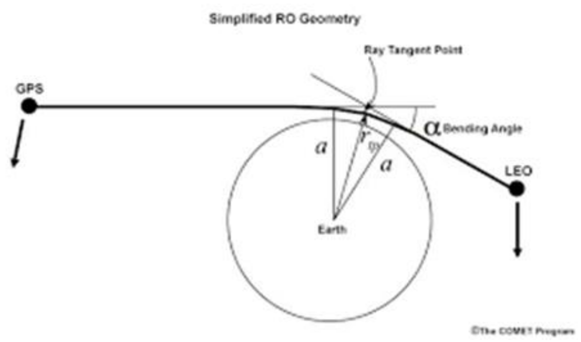

The change of delay of the signal allows for derivation of the bending angle, α and the vertical refractivity profile at the ray tangent point. The refractivity is used to derive profiles of ionospheric electron density near the tangent point. A similar technique is used to derive electron density from the ground-based RNSS observations, although in that case the path between satellite and the ground station is approximately perpendicular to the Earth's surface.

2.1.1.1 RNSS System 1A

This system generates ultra-low noise scintillation indices and RNSS measurements while logging and streaming data at up to 100 Hz, providing real time output of TEC and scintillation indices.

The Global Positioning System receiver tracks all visible GPS signals at the L1 frequency (1 575.42 MHz) and the L2 frequency (1 227.6 MHz). It measures phase and amplitude (at a 50-Hz or 100-Hz rate) and code/carrier divergence (at 1-Hz rate) for each satellite being tracked on L1 and L2 TEC is computed from combined L1 and L2 pseudorange and carrier phase measurements. Technical specifications for RNSS System 1A appear in Table 4.

2.1.1.2 RNSS System 1B

Approximately 20 of this type of RNSS receiver are deployed by the China Meteorological Administration (CMA), mainly in southern China where ionospheric scintillation occurs frequently. The most northern station is Mohe in Heilongjiang province, the most southern station is Xuwen in Guangdong province.

The receiver receives RNSS signals, analyses the amplitude and phase change information of the signal, and calculates the amplitude scintillation index, the phase scintillation index, and the TEC index. The receiver workstation calculates the ionospheric scintillation parameters, including amplitude scintillation S4 index, phase scintillation index, TEC, etc. Technical specifications of RNSS System 1B appear In Table 4.

2.1.2 Radio absorption

Ground-based measurements of radio signals from known sources above the atmosphere (usually cosmic radio sources) can be used to map the absorption in the lower ionosphere by using relative ionospheric opacity metres, or riometrers. The three most common types of radio wave absorption are:

1) auroral absorption caused by precipitating electrons, polar cap absorption;
2) associated with >10 MeV protons in the near-earth environment; and
3) X-ray induced absorption caused by solar X-ray bursts that generate an anomalous level of electrons in the D-region (typically 60-100 km altitude).

As the Earth rotates, radio sources move across the observer, and integrated flux is used to map the distribution of absorbing ionisation in the lower ionosphere. However, during periods of abnormal solar radio noise, the radio receiver can be saturated indicating solar radio noise activity. The current deployment density of ground-based observation sites is low.

2.1.2.1 Relative Ionospheric Opacity Meters for Extra-Terrestrial Emissions of Radio noise (riometers)

Ground based riometers measure the power of the background cosmic radio noise (from many radio stars), which is absorbed in the ionospheric D region (typically 60-100 km altitude). The D-region absorption is a function of the degree of ionization (electron density) present. In order to obtain the amount of absorption due to excess ionization, the measurement of any given day is subtracted from the so-called Quiet-Day Curve (QDC). The QDC is determined during selected days (typically during the month prior to the measurement) when there are no geomagnetic disturbances, i.e. the conditions are said to be geomagnetically quiet. This method therefore does not require the instrument to be absolutely calibrated, since the reference curve, i.e. the QDC, is obtained with the same instrument in close temporal proximity.

A riometer is a type of continuous wave (CW) radio receiver with receive sensitivity at the noise temperature of background sky and is designed to measure the absorption of radio waves that traverse the ionosphere. Typically, a twin-dipole antenna is orientated to the zenith resulting in a beam that has a diameter of ~100 km at the 90 km atmospheric altitude. For most of the time, the received RF level is dominated by radio emissions of galactic origin and has a regular variation in sidereal time that can be characterized with a quiet-day curve. Absorption of radio waves by the ionosphere reduces the voltage level (V) of the riometer to less than that of the quiet-day curve (Vqdc). The level of absorption is computed with the equation 10 log(Vqdc/V) dB each second. Figure 4 depicts the key element of riometer operation.

FIGURE 4

How a Riometer works

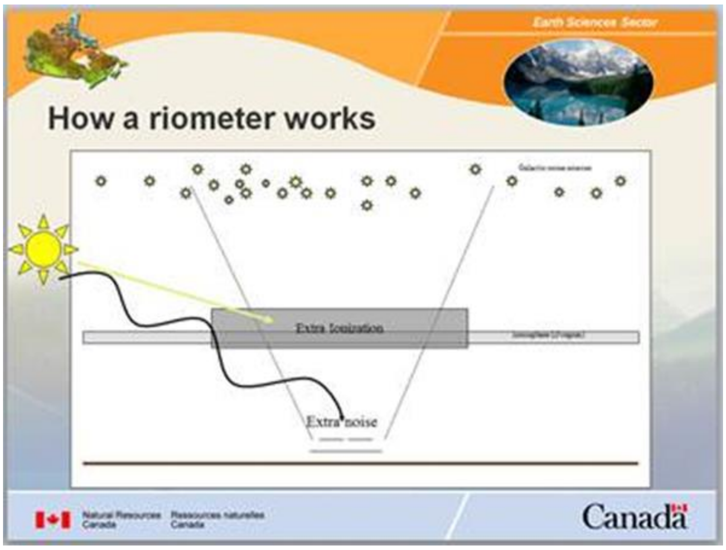

Multiple riometers can give some general background information for the near-Earth environment and the extent of the atmospheric absorption region.

The broad-beam riometers operate at 20.5, 30, 38.2, and 51.4 MHz. All except the 38.2-MHz instrument use linearly polarized double-dipole antennas; the 38.2-MHz instrument employs a circularly polarized crossed-dipole antenna. Since ionospheric absorption is inversely proportional to the square of the radio frequency, the operating frequencies are chosen to ensure that the radio waves are high enough in frequency to penetrate the ionosphere, yet low enough in frequency to be sensitive to ionospheric absorption.

There are approximately 50 riometer sites around the world, and most of these are located at high latitudes.

The above details mainly apply to riometers in the Global Riometer Array (GloRiA). GloRiA riometers are globally distributed, with a concentration in the auroral and polar zones. The technical details for the GloRiA riometers appear in Table 8 under “System 5A”. Other riometers exist at other locations around the world, including Antarctica, Australia, Argentina, U.S.A., S. Africa, Finland, Norway, Sweden, Russia, China, Greenland and Iceland. Details for these appear in Table 8 under “System 5B”.

2.1.2.2 Radio telescopes for ionospheric observation

Radio telescopes can be used to observe both the ionosphere and the solar wind (and details of the latter application appear in § 2.2.1).

Wide-bandwidth observations can identify ionospheric scintillation, leading to improved monitoring of the mid-latitude ionosphere. In addition, the differential Faraday rotation due to the ionosphere provides a clean, independent measure of ionospheric fluctuations. Combining this information with data about the Earth's magnetic field can in principle provide the absolute ionospheric TEC. However, the uncertainty of the Earth's magnetic field strength is much larger than that of the differential Faraday rotation. Another technique currently under development to determine the absolute TEC is to use the Faraday rotation of polarised cosmic sources. Characteristics of the systems included in this section appear in Table 4.

2.1.2.2.1 LOFAR (LOw Frequency ARray) – System 1C

LOFAR is an omni-directional system consisting of a phased-array of antennas grouped into individual stations which can operate singly or as a combined system for interferometry. A core of 24 stations covering an area with a diameter of 4 km is situated near Exloo in the north-east Netherlands; 14 stations are distributed further afield across the Netherlands; 13 stations are situated internationally, with six across Germany, three in Poland, and one each in France, Ireland, Sweden and the UK. Another station will be deployed in Latvia in 2019.

At each station, the RF signal is received within up to three out of a total of four frequency ranges (10-90 MHz, 110-190 MHz, 170-230 MHz, and 210-250 MHz), digitised, and, typically, a poly-phase filter applied to divide the signal into channels of 195 kHz. The resulting data from each station are complex voltage dynamic spectra which can be converted to Stokes parameters for subsequent data reduction, or combined for interferometric imaging and/or to form narrow, high-sensitivity, "tied-array" beams. LOFAR is capable of the following measurements in support of space weather monitoring operations:

1) monitoring the solar dynamic spectra,

2) measuring solar wind speed globally, and

3) measurement of ionospheric scintillation dTEC and differential Faraday rotation.

Because of its solar observing capability, details of LOFAR are repeated in § 2.2.2.1 and Table 7 under System 4H.

2.1.2.2.2 NENUFAR (New Extension in Nançay Upgrading LOFAR) System 1D

NENUFAR is an omni-directional system that consists of 1824 crossed dipole antennas operating as an aperture array of 400 m diameter, plus 114 additional antennas deployed up to 3 km distance from one another, operating as an interferometer. The digital receiver allows resolution bandwidth from few Hz to 195 kHz in the 10-85 MHz frequency band. With an effective area of 62 000 m^2 at 30 MHz for the aperture array, NENUFAR is a high sensitivity, low frequency, telescope for operating in full polarization in the frequency range 10-85 MHz.

NENUFAR is a multi-purpose low frequency system capable to be operated in the research fields of atmospheric, ionospheric and solar physics.

The monitoring of the ionosphere (spatial and temporal variability, scintillations, opacity and turbulence) is based on observations in the time and frequency domains and with high data rate and spectral resolution, of known radio sources (Jupiter, Sun, and other powerful extra-terrestrial radio sources such as some distant stars).

Due to its solar observation capabilities, NENUFAR is also included in section 2.2.2.1 and Table 7 under System 4K.

2.1.3 Ionosonde

An ionosonde transmits a sweep of radio signals (pulsed or continuous wave (CW-chirp)) into the ionosphere. Echoes are returned where the radio frequency equals the local plasma frequency, which is proportional to the square root of the electron density. The peak frequency returned from each ionospheric layer is therefore a direct measure of the electron concentration. In contrast, the height of each layer is estimated from the time of flight of the radio signal assuming propagation through free space. Heights derived from ionosonde data are denoted by the prefix ‘h’, and are referred to as virtual heights. Since the plasma frequency (electron density) is altitude dependent and also time-dependent with geophysical conditions, ionosondes must span a significant frequency range (e.g. ~0.5 to 15 MHz). Altitude coverage is limited by the peak ionospheric cut-off frequency. Higher frequencies beyond the local plasma frequency can be used for oblique sounding up to 30 MHz. Modern research ionosondes can also be used to measure additional variables, most notably plasma velocities and the spectrum of gravity waves. Characteristics of the systems included in this section are provided in Table 5.

2.1.3.1 Lowell Ionosonde (System 2B)

The Lowell Ionosonde System is a high frequency (HF) ionosonde. Deployment of the instrument includes preparation of the antenna field that nominally accommodates 1) a dual crossed delta transmit antenna suspended from a single 30 m tower with 44 m × 44 m space requirement, and 2) a receive antenna array consisting of four 1.5 m tall crossed loop elements occupying an equilateral triangle space of 60 m side length. About 80 systems are currently in operation worldwide. A subset of the network data is represented in online data repositories of the Global Ionosphere Radio Observatory (GIRO). The locations of the sounders is shown in Fig. 5.

The system transmits low-power phase-coded 533 µs radio pulses of varying frequency in its operational range between 0.5 and 30 MHz to detect and evaluate signatures of their reflection in the ionosphere. Details of the antenna are provided in Fig. 6. Nominal signal processing includes adaptive excision of the strong narrowband RF interferers, complementary-code pulse compression, and coherent Doppler integration. Data products for operational space weather use include (a) ionogram-derived URSI-standard ionospheric characteristics, (b) vertical electron density profile (EDP) of the sub-peak ionosphere, (c) vector velocity of the overhead bulk plasma motion, and (d) Doppler skymaps of the ionosphere showing the angle of arrival, Doppler frequency, echo range, and wave polarization of the detected echoes. In the synchronized operation of two sounders, the instrument records and processes oblique incidence ionograms, and high-resolution Doppler frequency and angles of arrival for the detection/specification of traveling ionospheric disturbances (TIDs).

FIGURE 5

Ionosonde Deployment Locations for System 2B

FIGURE 6

System 2B Antenna Diagram

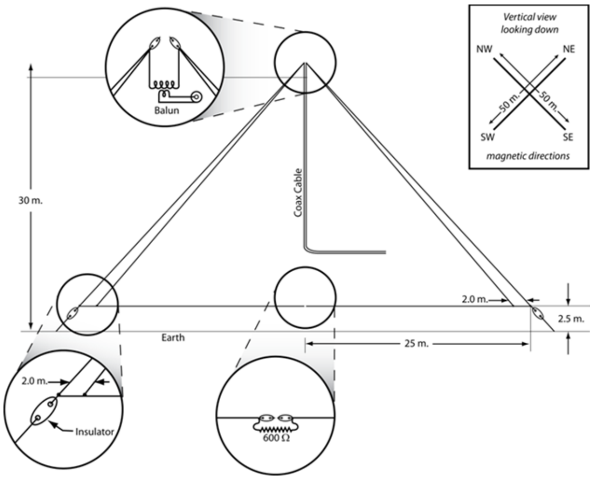

2.1.3.2 Chinese Ionosonde (System 2C)

Ionosonde System 2C is similar to System 2B with the exception of some differences in several operational characteristics. The transmitter is automatically tuneable over a wide range where typically the frequency coverage is 0.5-23 MHz or 1-40 MHz. The ionosonde pulses are reflected at various layers of the ionosphere, at heights of 100-400 km, and their echos are received and analysed by the control system. The result is displayed in the form of an ionogram showing the reflection height (actually time between transmission and reception of pulse) versus carrier frequency.

2.1.3.3 Finnish Ionosonde (System 2D)

System 2D works on a different principle than most other ionosondes. It uses a continuous-wave, frequency-modulated transmission (CW-chirp) instead of being a pulsed transmitter. It can therefore operate at lower power, nominally 150 W, but typically only 25 W or less are used. There’s no need for a T/R switch, but the receiver cannot be co-located with the transmitter. It is hence located about 1 km away. The only link between transmitter and receiver is precise timing. The receiver is an array consisting of 20 crossed loop aerials in five groups, arranged as an interferometric array, which will allow for determining the direction of arrival of the reflected wave from the ionosphere.

2.1.3.4 Mexican Ionosonde (System 2E)

Ionosondes installed in Mexico are similar to Finnish Ionosonde. They also use a continuous-wave, frequency-modulated transmission (CW-chirp) as a sounding signal within the HF range. The installed transceivers may be switched into transmitter or receiver modes. Possible ionospheric sounding modes are oblique (with the paths lengths 100-3 000 km) and quasi-vertical sounding (with the distance between a transmitter and receiver between 0.3-3 km). Transmitters can operate at power range (2-100) W; the typical output power is 10 W for vertical sounding and 100 W for oblique sounding. Dipole antenna are used. The raw results are displayed in the form of ionograms, which are processed to obtain the values of HF propagation parameters.

2.1.3.5 Advanced Ionospheric Sounder-Istituto Nazionale di Geofisica e Vulcanologia (AIS-INGV) – System 2F

Deployment of the AIS-INGV ionosonde includes preparation of an antenna field that nominally accommodates two delta antennas as transmitting and receiving antenna. They can be mounted on the same mast or on separate co-located masts. Dimensions are 25 m height x 40 m length.

Total number of AIS-INGV ionosondes operating all over the world are 4: 2 in Italy (Rome and Gibilmanna, Sicily) and 2 in Argentina (San Miguel de Tucuman and Bahia Blanca). There is another AIS-INGV ionosonde at Terra Nova Bay in Antarctica, however, it is currently not operative and expected to become operative until after 2019.

The AIS-INGV sounders operate by continuously sounding every 15 or 10 minutes and contribute to space weather services by providing real time monitoring of the electron density profile in the ionosphere. These sounders convey their measurements in the eSWua (electronic Space Weather upper atmosphere) data bank: http://eswuax.rm.ingv.it/.

The system transmits low-power phase-coded 480 µs radio pulses of varying frequency in its operational range between 1 and 20 MHz to detect their reflection in the ionosphere, allowing the evaluation of the ionosphere layers. The vertical resolution is about 4.5 km, in the range of altitude from 90 to 700 km.

Nominal signal processing includes adaptive reduction of strong narrowband RF interference emissions, complementary-code pulse compression, and coherent integration. Data products for operational space weather use include (a) ionogram-derived URSI-standard ionospheric characteristics, and (b) vertical electron density profile (EDP) of the sub-peak ionosphere.

2.1.4 Incoherent Scatter Radar

Incoherent scatter radar (ISR) is a radar technique for precise measurement of the thermal ionospheric plasma. The technique observes very weak scatter from thermal plasma ion-acoustic and Langmuir mode resonant oscillations. Primary measurements include electron density, electron temperature, ion temperature, and ionospheric drifts. A wide range of derived products are possible under certain conditions including electric fields, neutral winds, and ion compositions. Measurements are spatially resolved and can be made above and below the ionospheric peak.

While the height of ionospheric layers can be determined very accurately with ISRs, cross-calibration with ionosondes or the use of specific features in the ISR spectra are required to calibrate the electron concentration since the electron concentration is inferred from the total returned power. Estimates of the horizontal distribution of ionization can be obtained by moving the radar dish or by altering the phase of an antenna array. Vector velocities can be calculated by combining data from different antennas or from different beam directions.

The radars switch between multiple beams after each transmit pulse, and each beam is visited many times during a typical integration period of 15 to 60 s. The data from the multiple beams provide volumetric images of ionospheric electron density, electron temperature, ion temperature, and line-of-sight velocity. The line-of-sight velocities from multiple beams can be combined to produce estimates of the vector electric fields E-region neutral winds. ISRs transmit powerful VHF or UHF radio pulses into the ionosphere. Typical HF/VHF/UHF/L-band centre frequencies are used with up to 30 MHz bandwidth on receive and typically up to 1 MHz bandwidth on transmit for existing systems. Up to 10 MHz transmit bandwidth is planned for future systems. Significant power is required with most systems being multi-megawatt class with antennas between 25 and 300 meters in size. The high power is needed due to the very weak radar cross-section of thermal ionospheric plasma. Older systems are typically single antenna (parabolic reflector) based, with more modern systems having phased array radar antenna designs.

The following subsections provide information of some of the ISRs deployed throughout the world. Characteristics of the systems included in this section are provided in Table 5.

2.1.4.1 Millstone Hill ISR (System 2G)

The Millstone Hill Geospace Facility (MHGF) is located at the Massachusetts Institute of Technology (MIT) Haystack Observatory in Westford, Massachusetts, USA. This radar system consists of two 2.5 MW UHF klystron-based transmitters, a fully steerable 46 metre diameter antenna with a wide field of view. The radar produces full atmospheric altitude profiles of the plasma state at approximate kilometre scale resolution and 30-120 second time resolution over more than 3 hours of time and 30-40 degrees magnetic latitude. Millstone Hill also has a fixed zenith directed 68 meter diameter antenna for sensitive vertical ionospheric profiles.

The full steerability of the Millstone Hill ISR provides a capability for ionospheric observations encompassing the full extent of mid-latitude, sub-auroral, and auroral features and processes. For nearly six solar cycles, Millstone Hill’s location has made it a key enabling anchor for mid-latitude and sub-auroral community science in the important plasmasphere boundary layer (PBL). The availability of wide field, full altitude profiles of the plasma state across the eastern continental US using the incoherent scatter technique has led to many fundamental discoveries of complex coupling phenomena in the geospace system; the region of outer space near Earth, including the upper atmosphere, ionosphere and magnetosphere.

2.1.4.2 Poker Flat Incoherent Scatter Radar (System 2H)

The Poker Flat Incoherent Scatter Radar (PFISR) is an electronically steerable active phased array radar consisting of 4096 individual antenna element units. PFISR operates continuously and unmanned. The high duty-cycle modes of operation are customized for a variety of different scientific purposes, including studies of auroral electrodynamics, ionospheric structure and its impacts on radio propagation, particle precipitation and loss of particles from the radiation belts, auroral ion upflow, and atmosphere-ionosphere coupling through atmospheric waves.

2.1.4.3 Resolute Bay Incoherent Scatter Radar (RISR) – System 2I

The Resolute Bay Incoherent Scatter Radar – North (RISR-N) is an electronically steerable active phased array radar consisting of 3 872 individual antenna element units. RISR-N and its southward pointing sister radar, RISR-C (operated by the University of Calgary) are located at the Resolute Bay Observatory in Nunavut, Canada. Due to limited power production capabilities, operations are limited to campaigns of approximately eight days per month.

2.1.4.4 EISCAT (Systems 2J-2N)

EISCAT incoherent scatter radars are located in northern Norway, Finland, Sweden, and on Svalbard. The transmitters and transmit/receive antennas for the mainland systems are located in Ramfjordmoen, near Tromsø, Norway. Receivers and receive antennas are located in Kiruna, Sweden and Sodankylä, Finland. The Svalbard transmit and receive systems are located in Longyearbyen. EISCAT uses the incoherent scatter radar technique to probe the high-latitude ionosphere. The EISCAT antennas are reflector-based with narrow (on the order of 1 degree) beam widths and the systems use pulsed signals and phase-shift modulation to measure plasma parameters as functions of space and time. The systems can, depending on conditions, measure ionospheric plasma density, electron and ion temperatures, and ion velocity profiles from approximately 60 to several hundred kilometres altitude.

2.1.4.5 EISCAT_3D (Systems 2O, 2P)

EISCAT_3D uses the incoherent scatter radar technique to probe the high-latitude ionosphere and atmosphere. The EISCAT_3D antennas are active phased arrays with narrow (on the order of 1 degree) primary beam widths, advanced interferometry capabilities (for approximately 0.1 degree resolution), and the systems use pulsed signals and amplitude- and phase-shift modulation to measure plasma parameters as functions of space and time. The systems will, depending on conditions, measure ionospheric plasma density, electron and ion temperatures, and vector ion velocity profiles from approximately 60 to over 1 000 kilometres altitude.

This system is planned for deployment of the main transmit/receive site near Skibotn, Norway (System 2O) and for primarily receive sites near Karesuvanto, Finland and Kaiseniemi, Sweden (System 2P).

2.1.5 Coherent scatter radar

These radar systems measure coherent scatter from ionospheric irregularities due to plasma instabilities, waves and structures. In this way, the returned power and line-of-sight velocity can be determined. Vector velocities can be calculated by combining data from two or more radar stations. Coherent scatter radars have often been deployed as transportable systems which can be moved to allow for the study of different regions of the ionosphere. Typically, dedicated systems are developed at 30, 50, or 144 MHz with bandwidths in the 1 MHz range. The characteristics of the systems appearing in this section are provided in Table 5.

2.1.5.1 Super Dual Auroral Radar Network (SuperDARN) – System 2A

The SuperDARN is an international scientific radar network consisting of more than 32 high frequency (HF) radars located in both the Northern and Southern Hemispheres. The radars monitor the Earth’s upper atmosphere beginning at mid-latitudes and extending into the Polar Regions. SuperDARN radars typically operate in the HF band between 8.0 MHz and 20.0 MHz (the actual operational frequency bands for each radar are determined by the local radio licensing authorities). In the standard operating mode each radar scans through 16 beams of azimuthal separation of approximately 3.24°, with a scan taking 1 min to complete (approximately 3 seconds integration time per beam). The distance each beam covers is divided into 75 to 100 sections (range gates) each

45 km in distance, and so in each full scan the radars each cover 52° in azimuth and over 3 000 km in range; encompassing an area on the order of 1 million square km.

There are two types of antennas normally used. One type is a standard log-periodic antenna on a boom with back reflectors. The other type, which has become more prevalent in recent years, is the twin-terminated folded dipole, with a reflector made up of varying numbers of horizontal wires. The performance of both antennas is typically similar, although the latter type may have an improved front to back ratio, although this is dependent on the number of horizontal wires in the reflector.

The radars measure the Doppler velocity (and other related characteristics) of plasma density irregularities in the ionosphere. The radars operate continuously and observe the motion of charged particles (plasma) in the ionosphere and other effects that provide information on Earth's space environment.

TABLE 1

SuperDARN radar locations

Station name	Location	Latitude/ Longitude	Antenna boresight bearing	Operating Administration
King Salmon	King Salmon, Alaska, United States	58.6918°N 156.6588°W	340.0°	Japan
Hokkaido East	Hokkaido, Japan	43.5318°N 143.6144°E	25.0°	
Hokkaido West		43.54°N 143.6144°E	330.0°	
Syowa South	Showa Station, Antarctica	69.0108°S 39.5900°E	159.0°	
Syowa East		69.0085°S 39.6003°E	106.5°	
Adak Island East	Adak Island, Alaska, United States	51.8929°N 176.6285°W	46.0°	United States
Adak Island West		51.8931°N 176.6310°W	332.0°	
Kodiak	Kodiak, Alaska, United States	57.6119°N 152.1914°W	30.0°	
Blackstone	Blackstone, Virginia, USA	37.1019°N 77.9502°W	320.0°	
Fort Hays East	Hays, Kansas, United States	38.8585°N 99.3886°W	45.0°	
Fort Hays West		38.8588°N 99.3904°W	335.0°	
Goose Bay	Happy Valley-Goose Bay, Newfoundland and Labrador, Canada	53.3179°N 60.4642°W	5.0°	
Kapuskasing	Kapuskasing, Ontario, Canada	49.3929°N 82.3219°W	348.0°	
Wallops Island	Wallops Island, Virginia, United States	37.8576°N 75.5099°W	35.9°	

TABLE 1 (*end*)

Station name	Location	Latitude/ Longitude	Antenna boresight bearing	Operating Administration
Christmas Valley East	Christmas Valley, Oregon, United States	43.2703°N 120.3567°W	54.0°	
Christmas Valley West		43.2707°N 120.3585°W	340.0°	
McMurdo	McMurdo Station, Antarctica	77.8376°S 166.6559°E	300.0°	
South Pole	South Pole Station, Antarctica	89.995°S 118.291°E	75.7°	
Prince George	Prince George, British Columbia, Canada	53.9812°N 122.5920°W	355.0°	Canada
Saskatoon	Saskatoon, Saskatchewan, Canada	52.1572°N 106.5305°W	23.1°	
Rankin Inlet	Rankin Inlet, Nunavut, Canada	62.8281°N 92.1130°W	5.7°	
Inuvik	Inuvik, Northwest Territories, Canada	68.4129°N 133.7690°W	26.4°	
Clyde River	Clyde River, Nunavut, Canada	70.49°N 68.50°W	304.4°	
Stokkseyri	Stokkseyri, Iceland	63.8603°N 21.0310°W	301.0°	United Kingdom
Thykkvibaer Cutlass/Iceland	Thykkvibaer, Iceland	63.7728°N 20.5445°W	30.0°	
Hankasalmi Cutlass/Finland	Hankasalmi, Finland	62.3140°N 26.6054°E	348.0°	
Halley*	Halley Research Station, Antarctica	75.6200°S 26.2192°W	165.0°	
Dome C	Concordia Station, Antarctica	75.090°S 123.350°E	115.0°	Italy
SANAE	SANAE IV, Vesleskarvet, Antarctica	71.6769°S 2.8282°W	173.2°	South Africa
Kerguelen	Kerguelen Islands	49.3505°S 70.2664°E	168.0°	France
TIGER	Bruny Island, Tasmania, Australia	43.3998°S 147.2162°E	180.0°	Australia
TIGER-Unwin	Awarua, near Invercargill, New Zealand	46.5131°S 168.3762°E	227.9°	
Zhongshan	Zhongshan Station, Antarctica	69.3766°S 76.3681°E	72.5°	China
Longyearbyen	Svalbard, Norway	78.153°N 16.074°E	23.7°	Norway
Buckland Park	Buckland Park, Australia	34.620°S 138.460°E	146.5°	Australia
Falkland Islands	Falkland Islands, South Atlantic	51.83°S 58.98°W	178.2°	United Kingdom

2.1.5.2 Middle Atmosphere Alomar Radar System (MAARSY) (System 2Q)

MAARSY is a radar for improved studies of the Arctic atmosphere from the troposphere up to the lower thermosphere with high spatio-temporal resolution. It is based at Andøya (69.30°N, 16.04°E), Norway. MAARSY will have the capability to conduct ionospheric incoherent scatter observations after a planned upgrade of the MAARSY antenna array to circular polarization is complete.

FIGURE 7

MAARSY Antenna Array

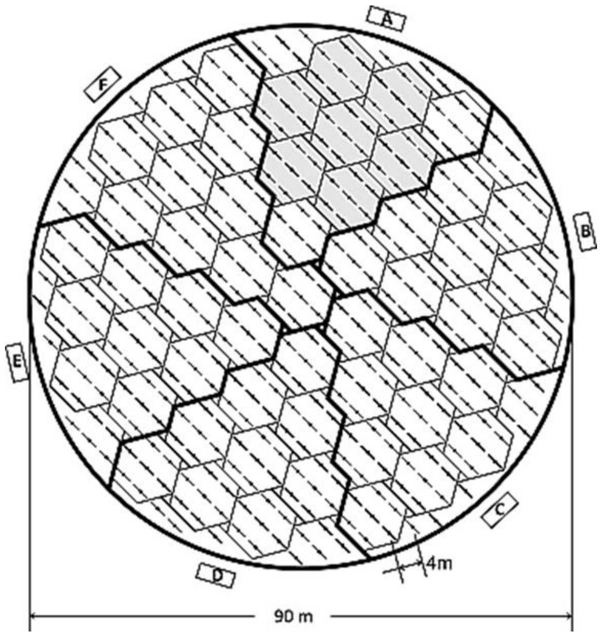

Figure 7 shows a diagram of the MAARSY antenna array. The 90 metre array is comprised of 61 subarrays. Fifty-five of the subarrays are hexagonal arrays of 7 antennas. In addition, there are 6 asymmetric arrays of 8 antennas. The boxes shown around the array perimeter are equipment shelters.

2.1.6 Other Radar Systems

2.1.6.1 HF Doppler System

An HF Doppler system consists of a CW radio transmitter and several receivers, which are highly frequency stable combined with a recording device. The CW signals are typically transmitted at frequencies between 3 and 10 MHz. When a radio wave is reflected from the ionosphere, a movement of the reflection point will produce a change in signal phase path and hence a Doppler shift proportional to the time rate of change of the path. If three or more spatially separated propagation paths are monitored, the time difference of the TID signatures at the reflection points yields the speed and direction of the TID by triangulation.

HF Doppler measurements can be used to study: ionospheric disturbances such as atmospheric gravity waves (AGW), TID, ionospheric sporadic E and spread F layer occurrences, as well as magnetic pulsation ultra-low frequency (ULF) waves such as Pi2 pulsations[1]. Understanding TID

[1] Pi2 pulsations are irregular, damped ULF range magnetic pulsations occurring in connection with magnetospheric substorms.

and AGW characteristics are important in space weather monitoring since the propagation of ionospheric scintillations caused by these phenomena allows short-time forecasting of the impacts of space weather on radio-communications and RNSS reliant applications. Sufficient details of characteristics of HF Doppler systems are not available at this time for inclusion in Table 5.

2.1.6.2 Mesosphere/lower thermosphere (MLT) dynamics radars

These systems provide measurements of the mesosphere regions through partial reflection observations, often augmented with Faraday rotation. The mesosphere is a crucial atmospheric layer and is relatively quite difficult to observe this region by techniques other than meteor radar (MR) and medium frequency (MF) radar. These radar measurements of the MLT have widely been used to detect mean winds and tides, and to get insight into the seasonal, interannual, and long-term behaviour of the MLT circulation including long-term trends. In addition, MR and MF radar wind measurements have been combined to analyse properties of planetary waves, and to construct empirical climatologies of MLT wind parameters. Sufficient details of characteristics of MLT dynamics radar are not available at this time for inclusion in Table 5.

2.1.7 Ionospheric Tomography

Ionospheric tomography is a technique for atmospheric electron density analysis in the two or three-dimensional domain. The method is based on ground-based measurements of low Earth orbit (LEO) satellite dual-frequency signals of 150 and 400 MHz. Dual-frequency radio receivers measure the phase difference of signals transmitted by the satellites. Several receivers are required for tomographic analysis, but also measurements from individual receivers are used for ionospheric studies. Depending on the algorithm in use, electron density measurements from other instruments (e.g. from RNSS receivers) can be used in addition. Characteristics of the systems appearing in this section are provided in Table 5.

2.1.7.1 TomoScand network of Beacon receivers (System 2R)

The TomoScand receiver network consists of 14 receivers located in Norway, Estonia, Sweden and Finland. There are similar receiver networks operating around the world, including operations in West and East Russia, and South-East Asia (Thailand, Philippines, Indonesia, Vietnam and China). The satellites used for this purpose are navigation satellites, such as the Russian COSMOS satellite, or the transmitters are built specifically for ionospheric studies as in the Canadian CAScade, Smallsat and IOnospheric Polar Explorer (CASSIOPE) satellite and in the recently launched China Seismo-Electromagnetic Satellite (CSES) mission. With the advent of affordable miniaturized satellites, such as cubesats, the amount of available transmitters is expected to increase.

As the free electrons in the atmosphere cause phase shifts to the propagating electromagnetic waves, the measured phase differences can be used to derive the TEC along the signal path. TEC measurements from multiple receiver stations enable the use of tomographic methods to reconstruct two or three-dimensional electron density distributions. The frequencies used are established as standards in LEO based tomography, and there are several satellites transmitting these frequencies. The existing receiver technology has been developed for these frequencies. Compared to RNSS satellites, the lower frequencies are more sensitive and better suited for detecting small scale variations in TEC as they rapidly sweep over extensive latitude ranges. In addition, many LEO satellites are on polar orbits, providing measurements from high latitudes, whereas inclinations of RNSS satellites are limited to 55 degrees with GPS and to 65 degrees with Globalnaya Navigazionnaya Sputnikovaya Sistema (GLONASS). It is important to note that LEO satellite measurements provide significantly different type of measurements in comparison to RNSS and should be seen as complementary systems.

The tomographic method is unique as the ionospheric reconstructions are mesoscale 3D electron densities of a larger domain than individual instruments can typically provide. It provides cost-effective near real-time ionospheric observations that can be utilised to improve satellite positioning and high-frequency radio communication. The goal is to integrate a quick look version of TomoScand to operational services during coming years.

Additional information: http://www.space.fmi.fi/MIRACLE/tomoscand/.

2.1.8 Antarctic-Arctic Radiation-belt (Dynamic) Deposition – VLF Atmospheric Research Konsortium (AARDDVARK)

One of the few techniques that can probe the ionospheric D-region uses very low-frequency (VLF) electromagnetic radiation trapped between the lower ionosphere (approximately 85 km) and the Earth; these signals can be received thousands of kilometres from the source. The nature of the received radio waves is determined by propagation inside the Earth-ionosphere waveguide, with variability largely coming from changes in the electron density profiles at and below the lower ionosphere (the D-region). During solar flares, these D-region electron densities are driven, in large part, by soft (1-10 keV) X-rays from the flare itself. Hence, these observations produce an indirect observation of the nature of the solar flare.

The AARDDVARK global-scale network of sensors monitors fixed-frequency communications transmitters, and hence provide continuous long-range observations between the transmitter and receiver locations.

The receivers record small changes in the phase and amplitude of the VLF communications transmitters (~13-45 kHz). By monitoring distant VLF stations, long-range remote sensing of these changes, particularly in the lower ionosphere are achieved. The receivers are primarily located in the Polar Regions (both the Antarctic and Arctic), but some are located in mid-latitudes as well. A schematic depiction of the subionospheric VLF propagation is shown in Figure 8. There are about currently 20 stations. The locations of some of the current stations are listed below while all the locations are shown in Figure 9. The characteristics of the AARDDVARK network are provided in Table 9.

Antarctica: Halley, Rothera, Scott Base, SANAE, Casey, Davis

Canada: Fort Churchill, Edmonton, Ottawa, St John’s

New Zealand: Dunedin

Hungary: Erd

Finland: Sodankylä

Norway: Ny Alesund

Scotland: Eskdalemuir

USA: Forks, Fairbanks

Iceland: Reykjavik

UK: Ascension Island

FIGURE 8

Schematic of subionospheric VLF propagation. VLF transmissions propagate in the waveguide formed by the Earth and the lower edge of the ionosphere (for night time ~85 km)

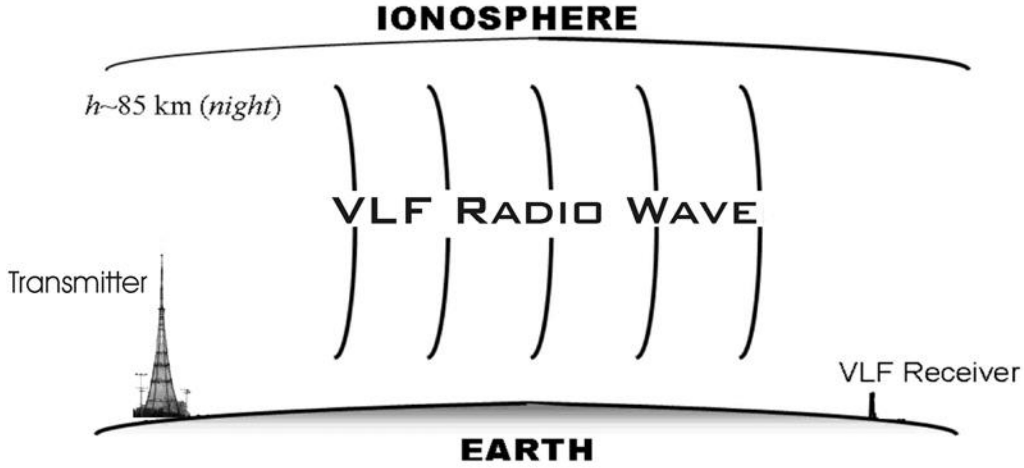

FIGURE 9

AARDDVARK summary. Receivers are the red diamonds, VLF transmitters the green circles, and the great circle paths joining them are shown as black lines

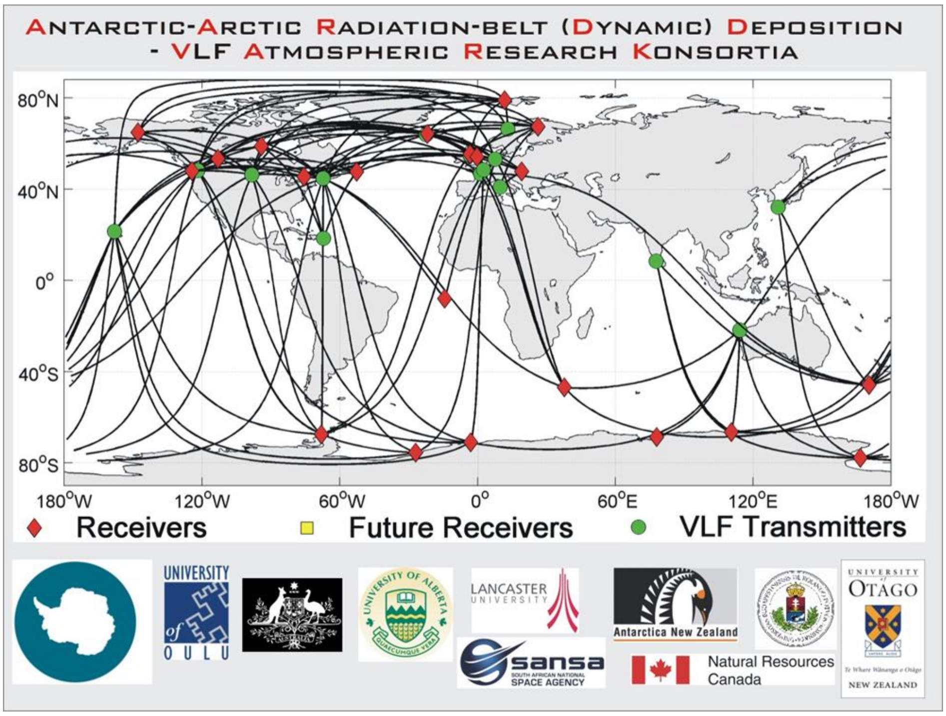

2.2 Solar observations

Solar observations are obtained from a combination of ground-based and space-based instruments. Such observations include solar active region characteristics, flare properties, radio emissions, coronal structure and photospheric magnetic field attributes.

Solar radio emissions are observed with ground-based radio frequency spectrographs, imagers and single-frequency solar radio flux monitors. No space-based RF solar observation sensors have been identified for inclusion in this report at this time.

Radio observations are provided by:

1) spectrographs that observe the full Sun over an extended frequency range,

2) single antennas that observe the full Sun at selected frequencies, and

3) imagers based on the technique of aperture synthesis (interferometry).

The spectrographs are particularly useful for observing solar radio bursts that are indicators of flares, CMEs, and other solar phenomena. The classification types and characteristics of these radio bursts is provided in Table 2. Figure 10 shows the typical radio spectrum history for a solar flare and further details of the distribution of flux density versus wavelength for a range of large radio bursts appear in Fig. 12.

Single-frequency flux measurements can be used to observe the solar wind and track CMEs using interplanetary scintillation, and to monitor solar radiation at various frequencies. A solar radio flux parameter, called F10.7, is a measurement of solar radio emission at a wavelength of 10.7 cm. This solar radio flux is highly correlated with sunspot number, and its recorded measurements provide a key database both for driving space weather models and for understanding the multiannual variations of the Sun. Imagers at radio wavelengths localize the burst sources and provide measurements of the electron density and electron temperature in the quiet (thermal) solar atmosphere.

Figure 10 presents the overall spectrum history of a solar flare observed in radio frequencies. Following the initial impulsive start of the flare, which is observed at most frequencies, the material around the flare heats and propagates outward into the thinner atmosphere characterized by emissions at lower frequencies. The emission profiles typically observed at discrete frequencies are as shown on Fig. 11.

FIGURE 10

Typical radio spectrum history for a large solar flare

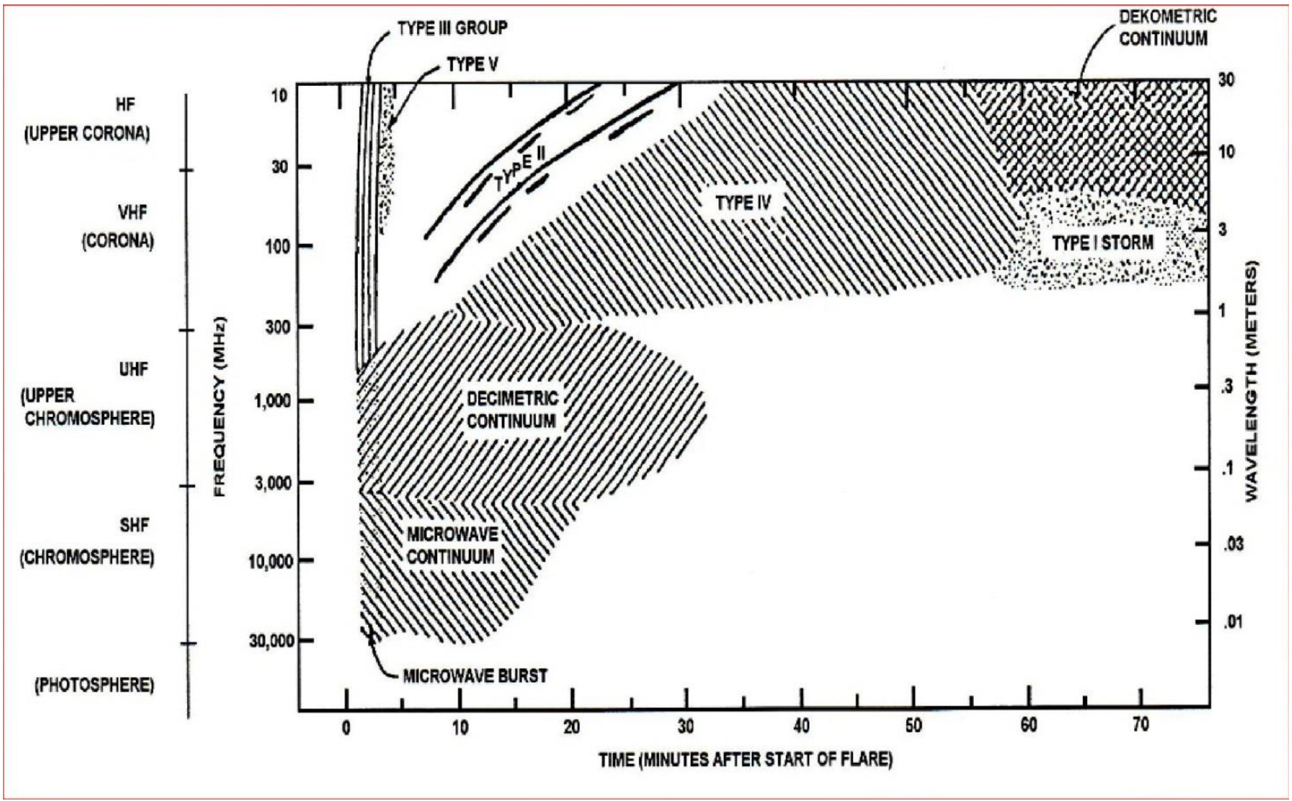

FIGURE 11

Emission profile of a typical solar radio flare

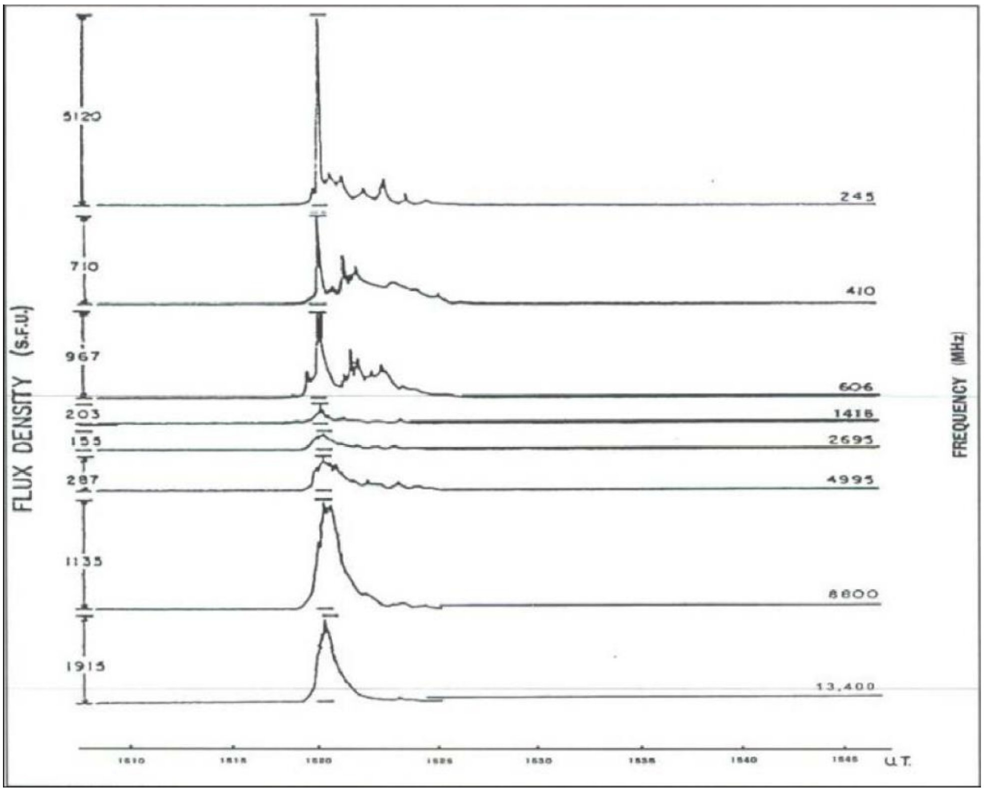

FIGURE 12

Exemplary solar radio fluxes

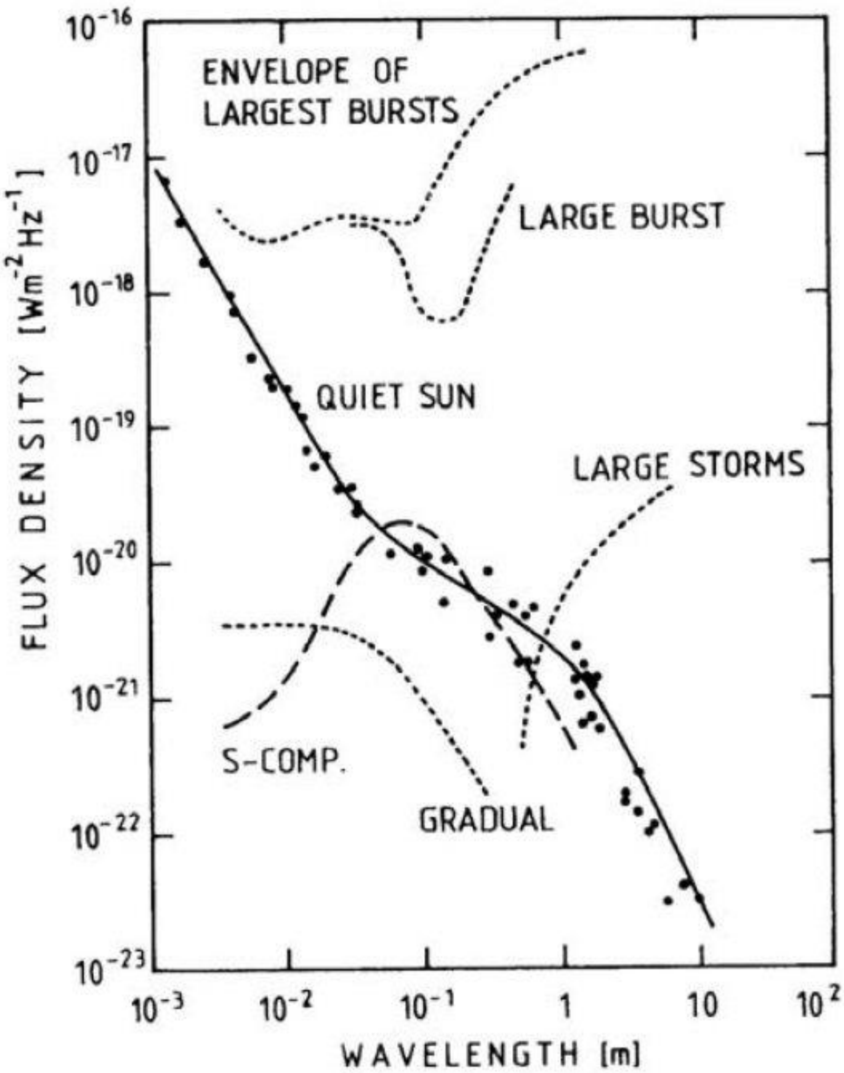

The radio fluxes associated with the quiet sun and the envelopes of various solar flares are shown on Fig. 12. The character of the solar flare emissions at lower radio frequencies and the associated solar phenomena are given on Table 2. The solar radio flux associated with the quiet sun is illustrated on Fig. 13.

TABLE 2

Characteristics of solar radio flares

Type	Characteristics	Duration	Frequency range	Associated phenomena
I	Short, narrow-bandwidth	Burst: ~ 1 sec. Storm: hours-days	80-200 MHz	Active regions, flares, eruptive Prominences
II	Slow frequency drifts from high to low frequencies, usually with a strong second harmonic	3-30 min.	Fundamental: 20-150 MHz	Flares, proton emission, shockwaves moving upward exciting radio emissions at the plasma frequency
III	Fast frequency drifts from high to low frequencies, frequently with a second harmonic	Burst: 1-3 sec. Group: 1-5 min.	10 kHz – 1 GHz	Active regions, flares, electron beams propagating upward exciting radio emissions at the plasma frequency
IV	Broadband continuum, may drift from high to low frequencies	Hours-Days	20 MHz – 2 GHz	Flares, proton emissions
V	Smooth, short-lived continuum. Follow type III bursts	1-3 min.	10-200 MHz	Active regions, Flares

These solar radio emissions are monitored by ground-based radio observatories. At these observatories, the position of the sun is a function of the time of day (horizon to horizon), the day of year (driven by the tilt of the Earth’s axis), and the latitude of the observatory. The position of the sun varies over the course of the observation, which lasts for many hours rather than a few minutes.

The minimum solar radio flux has been observed historically at the minimum of solar activity. The solar radio flux spectrum at the minimum of the solar cycle is shown in Fig. 13, where Radio Solar Telescope Network (RSTN) and Nobeyama Radio Polarimeter (NoRP) are data from two different observatories. The solar radio flux observations are reported in units of solar flux units, where one solar flux unit (SFU) = 10^{-22} watt per square meter-hertz, or 10 000 Jansky.

FIGURE 13

Solar minimum radio flux spectrum

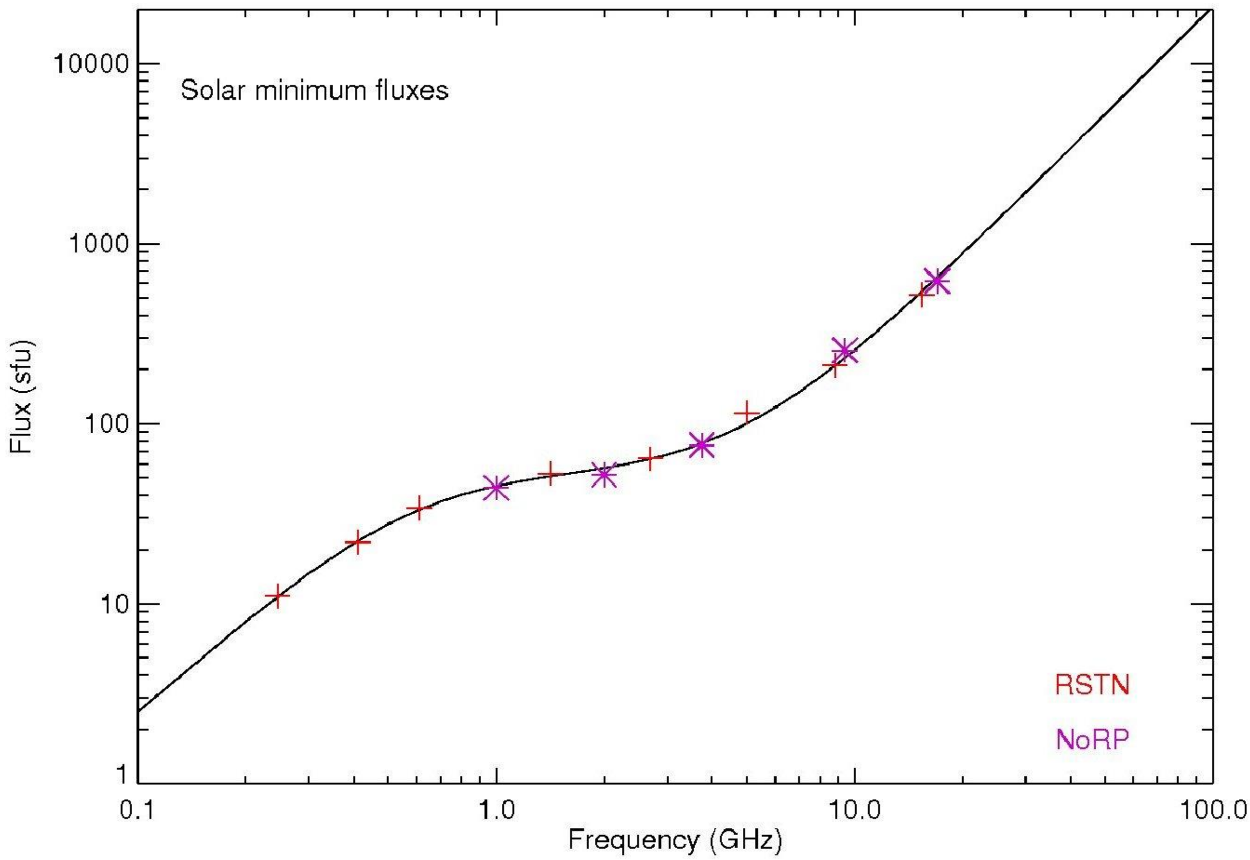

The allowable interference from all non-solar sources can be determined from the accuracy and precision requirements of the observed data rather than derived from the receiver parameters. The needed parameters are the observed solar flux, the level of precision needed (typically three digits), and the bandwidth being observed. The allowable interfering flux can be calculated using the equation below:

$$I_{max} = SolarRadioFlux_{min} \times Bandwidth \times Precision$$

where:

I_{max} = maximum acceptable interference level

$SolarRadioFlux_{min}$ = typical solar radio flux observed at solar minimum

Bandwidth = bandwidth of the receiver

Precision = precision of the measurement, typically 3 digits, or −30 dB.

Thus, the allowable interfering flux is determined from the observed data rather than derived from the receiver parameters.

Figure 14 shows a generic diagram of a multi-frequency solar flux monitoring system.

FIGURE 14

Generic diagram of a multi-frequency solar flux monitor system

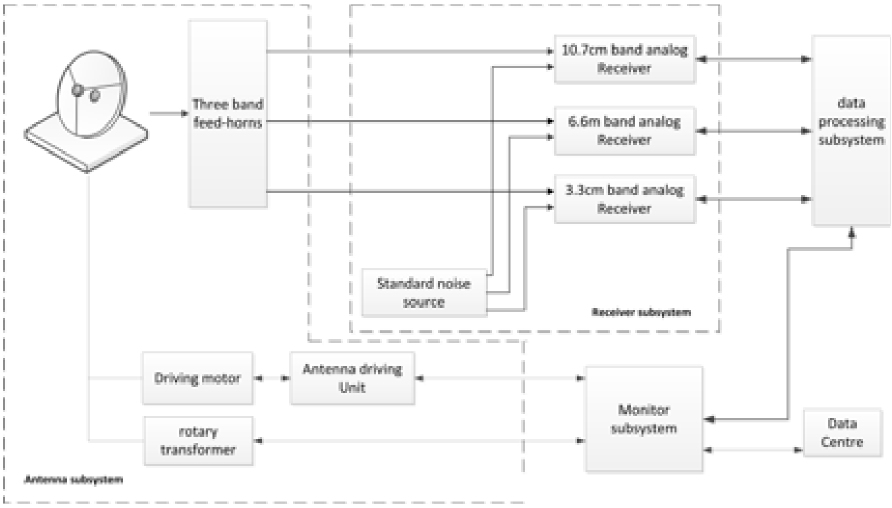

2.2.1 Spectrograph Observations

Radio emission observations, indicating the occurrence of radio bursts and the speed of shocks in the solar wind, are required with a stated cadence of 0.1 to 60 seconds (though a cadence of as long as 60 seconds is not particularly useful for radio bursts) and a delay of availability of 1 to about 30 minutes.

Solar radio observatories are deployed worldwide and provide 24-hour, 7-days a week coverage of solar radio emissions. Solar radio spectrographs typically sweep through a range of frequencies ranging from a few tens of MHz to a few GHz. Single frequency solar radio flux monitors operate in the frequency range from 150 MHz to 35 GHz. Characteristics of the systems appearing in this section are provided in Table 6.

2.2.1.1 Compound Astronomical Low-cost Low-frequency Instrument for Spectroscopy in Transportable Observatory (CALLISTO) System 3A

The CALLISTO instrument is a sweeping radio spectrometer operating between 45 and 870 MHz. Other frequency ranges can be observed by using either a heterodyne up- or down-converter. The CALLISTO instrument observes 825 MHz of the solar radio spectrum using individual channels which have a bandwidth of 300 kHz and can be tuned in 62.5 kHz increments. The narrow channel width and accurate positioning are essential to avoid known sources of interference. The number of channels per observing program is limited between 4 and 400, and up to 800 measurements can be made per second. For a typical number of 200 channels, the sampling time per channel is 0.25 seconds. CALLISTO instruments are easily transportable and used in many observatories. All collected data are freely available at the link: http://soleil.i4ds.ch/solarradio/callistoQuicklooks/.

The list of CALLISTO instruments already deployed worldwide, 155 instruments per April 2019, are listed below in Table 3. More detailed information as well as the last up-to-date list of CALLISTO instruments deployed worldwide can be found under the following link: http://www.e-callisto.org/Callisto_DataStatus_Vwww.pdf.

TABLE 3

CALLISTO stations worldwide

Country	Number of instruments	Antenna type	Frequency coverage
Algeria	2	Not Available	45-890 MHz
Australia	3	LPDA LPDA + tracker	45-890 MHz 100-850 MHz
Austria	5	LPDA, 3-band dipole LPDA crossed LPDA	20-80 MHz, 510-785 MHz 45-81 MHz, 45-890 MHz
Belgium	2	Dish 6 m	45-435 MHz
Brazil	2	LPDA linear polarization V, H	45-890 MHz
Bulgaria	1	LPDA	45-870 MHz
China	5	Not Available	45-890 MHz
Costa Rica	1	Dish	45-890 MHz
Czech Republic	1	Dish 7m	45-890 MHz
Denmark	4	LWA	10-105 MHz
Egypt	1	LPDA	45-890 MHz
Ethiopia	2	LPDA	45-890 MHz
Finland	4	LPDA LWA	45-890 MHz 5-120 MHz
France	1	Not Available	45-890 MHz
Germany	2	Bicone	20-80 MHz
Greenland	2	LWA	45-890 MHz
India	10	LPDA	45-410 MHz, 45-445 MHz, 45-870 MHz, 45-890 MHz
Indonesia	4	LPDA	45-405 MHz
Ireland	5	LPDA, Bicone, Inverted-V	45-890 MHz
Italy	4	LPDA	45-81 MHz, 220-425 MHz
Japan	5	LPDA	45-890 MHz
Kazakhstan	2	LPDA	45-165 MHz, 175-890 MHz
Kenya	1	LPDA	45-890 MHz
Malaysia	9	LPDA	45-890 MHz
Mauritius	3	LPDA	45-455 MHz, 45-890 MHz
Mexico	3	LPDA	45-890 MHz, 45-225 MHz
Mongolia	2	LPDA	45-890 MHz
Nepal	1	LPDA	45-870 MHz
New Zealand	1	Not Available	45-890 MHz
Norway	2	LPDA 8 dB	1 000-1 600 MHz
Pakistan	2	LPDA	45-890 MHz
Peru	2	LPDA	45-890 MHz

TABLE 3 (*end*)

Country	Number of instruments	Antenna type	Frequency coverage
Russian Federation	1	LPDA	45-440 MHz
Rwanda	1	LPDA	45-81 MHz
Slovakia	2	LPDA	45-200 MHz
South Africa	2	LPDA	45-890 MHz
South Korea	2	LPDA	45-445 MHz
Spain	5	LPDA	45-890 MHz
Sri Lanka	3	LPDA	45-890 MHz
Switzerland	14	Dish 5 m Dish 7 m LWA BICONE, LPDA LWA LHCP and RHCP	10-80 MHz, 1 415-1 430 MHz 45-81 MHz, 1 580-1 650 MHz 10-80 MHz, 150-870 MHz 15-90 MHz
Thailand	4	Not Available	45-890 MHz
Turkey	1	Not Available	45-890 MHz
Ukraine	1	16 Yagi-Array	250-350 MHz
United Kingdom	4	LPDA	45-81 MHz
Uruguay	2	LPDA	45-890 MHz
USA	21	LPDA, LWA LPDA vertical + sun track, LWA circular, Yagi vertical polarization LWA circular polarization	215-420 MHz 20-90 MHz, 90-305 MHz 45-93 MHz

2.2.1.2 Other Spectrograph Systems

Characteristics of the systems appearing in this section are provided in Table 6.

2.2.1.2.1 Nançay Decameter Array (NDA) – System 3B

The NDA is composed of 144 log-periodic Tee-Pee antenna located within the radioastronomy station of Nançay, middle in the Sologne forest, France. The array is dedicated to routine observations of powerful radio sources typically within the 10-90 MHz range, namely Jupiter and the solar corona. As for Jupiter, the NDA tracks Jovian auroral decametric emissions between 10 and 40 MHz, some of which characterize the response of Jupiter’s magnetosphere to solar wind activity at 5 AU. The NDA tracks solar radio burst within the 10-90 MHz range of types II, III and IV (see Fig. 10 and Table 2) which are induced by energetic electrons propagating in the high corona (about 0.5 to 1 solar radius above the photosphere). NDA observations of these two targets have been performed on a daily basis since 1977 and made available to the community online.

Space-weather data are provided in near real-time to the French Air Force together with the Nançay Radioheliograph (NRH) and the Observation Radio Fréquences pour l’Etude des Eruptions Solaires (ORFEES) observations.

Webpage: https://www.obs-nancay.fr/-Reseau-decametrique-24-?lang=en.

2.2.1.2.2 Augmented Resolution CALLISTO Spectrometer (ARCAS) and Humain Solar Radio Spectrometer (HSRS) – System 3C and System 3J, respectively)

Both these instruments are operated by the Solar Influences Data Analysis Center (SIDC) in Belgium. ARCAS operates between 45 and 450 MHz, and HSRS between 275 and 1 496 MHz. Both are digital spectrometers based on a Software Defined Radio receiver, and ARCAS shares the same receiving antenna as the Belgian CALLISTO receiver via a splitter. HSRS is connected to a broad-band antenna located at the focal point of the 6-m dish.

2.2.1.2.3 Korean Spectrographs (systems 3D and 3E)

There are two spectrographs – one at Jeju operating between 30 and 500 MHz and one at Icheon operating between 30 and 2 500 MHz. The instruments use 10M and 6M parabolic antennas and LP antennas.

2.2.1.2.4 Acceleration, Reconnection, Turbulence and Electrodynamics of the Moon's Interaction with the Sun (ARTEMIS), Greece (System 3F)

ARTEMIS observations cover the frequency range from 20 to 650 MHz. The spectrograph has a 7-meter steerable parabolic antenna for 110 to 650 MHz and a fixed antenna for the 20 to 110 MHz. There are two receivers operating in parallel, one a sweep frequency receiver for the whole range (10 spectrums/sec, 630 channels/spectrum) and the other an acousto-optical receiver for the range 270 to 470 MHz (100 spectrums/sec, 128 channels/spectrum). More technical information is available at http://artemis-iv.phys.uoa.gr/ARTEMIS%20PRESENTATION%20FOR%20LOIS.htm.

2.2.1.2.5 Yamagawa, Japan (System 3G)

These observations cover the 70-9 000 MHz range. The system is designed for solar radio burst and solar flare monitoring and has been operational since 2016.

2.2.1.2.6 ORFEES, France (System 3H)

ORFEES is a solar-dedicated radio spectrograph developed by Paris Observatory with support by the French Air Force. It measures flux-densities of radio bursts in the solar low/middle corona (<0.5 solar radii above the surface) over the 140-1 000 MHz range. The spectrograph is connected to a 5 m parabolic dish with a focal system composed of log-periodic dipoles. The spectrum is scanned ten times per second in five bands of 200 MHz bandwidth. The instrument is dedicated to the Sun, with daily observations between about 8:00 and 16:00~UT in summer, 8:30-15:30 UT in winter. Data are provided the day after the observation for scientific research via the web site http://secchirh.obspm.fr/index.php, which also offers a visualisation of other ground-based and space-borne solar radio observations. Space-weather data are provided in near real-time to the French Air Force together with the NRH and the NDA observations. Real-time data provision can also be developed for other space weather services. The data archive dates from 2012 to the present.

2.2.1.2.7 Radio Solar Telescope Network (RSTN) – Solar Radio Spectrograph (SRS)

The worldwide RSTN, a part of the Solar Electro-Optical Network (SEON) observing system, provides 24 hour a day, 7 day a week monitoring of the Sun. Radio telescopes are located in Learmonth, Australia, San Vito, Italy, and in the United States of America, in Sagamore Hill in Massachusetts, Holloman Air Force Base in New Mexico, and Kaena Point in Hawaii.

The RSTN system has two components: the SRS and the Radio Interference Monitoring Systems (RIMS), which monitors the sun at 8 discrete frequencies. The SRS monitors the frequency range of 18-180 MHz using two antennae, one to monitor the middle corona in a low band of 18-75 MHz and another to monitor the lower corona in a high band of 75-180 MHz. Sufficient details of characteristics of the SRS are not available at this time for inclusion in Table 4.

2.2.2 Discrete Observations

2.2.2.1 Interplanetary Scintillation (IPS)

IPS is the variation in the apparent intensity of radio waves from a distant, compact, radio source produced by variations in the density of the solar wind. This produces a drifting pattern of scintillation in the radio signal across the Earth and thus allows IPS to be used as a probe for investigating the inner heliosphere. Most observation systems that exploit IPS operate at single frequencies. The LOFAR system instead receives radio signals within 4 filter bands. LOFAR is included in this section since it also exploits the IPS technique. Characteristics of the systems appearing in this section are provided in Table 7.

2.2.2.1.1 LOFAR radio telescope (System 4H)

The LOFAR radio interferometer (see also § 2.1.2.2), with its antenna stations located in several countries in Europe, has unique capabilities for solar observations and space weather monitoring. Thanks to the combination of long and short distance baselines, LOFAR can observe the Sun with high spatial resolution at low frequencies (10-90 MHz and 110-190 MHz, 170-230 MHz, 210-250 MHz).

Due to the low frequencies at which LOFAR is observing, the measurements are sensitive to interplanetary scintillation. The observed interplanetary scintillation is a measure for the solar wind density and velocity. When observing compact cosmic sources with LOFAR's long baselines it is possible to resolve different solar wind streams. In this way it is possible to probe the solar wind at a short distance to the Sun. It should be noted that this technique is still in development.

2.2.2.1.2 Japan IPS (System 4I)

Japan operates an IPS system with antennas located at Toyokawa, Fuji, and Kiso. The solar wind speed is derived from the cross-correlation analysis between IPS signals detected at separated stations, and the global structure of the solar wind is retrieved from the tomographic analysis of IPS observations.

2.2.2.1.3 Mexican Array Radio Telescope (MEXART) IPS (System 4J)

MEXART (www.mexart.unam.mx) is a plane array of 64 × 64 (4096) full wavelength dipoles with an operation frequency of 139.6 MHz (2.1 m). The array is located at Coeneo, Michoacan (101°W 41' 39", 19°N 48' 49") and operates as a transit instrument fully dedicated to IPS observations. The solar wind speed is derived using a single-station methodology.

2.2.2.1.4 NENUFAR, France (System 4K)

NENUFAR (see also § 2.1.2.2) is a high sensitivity aperture array with additional antennas that form a 3 km baseline interferometer that has capabilities for solar observations and space weather monitoring.

NENUFAR will allow the study of the interplanetary medium through propagation phenomena and interplanetary scintillation.

2.2.2.2 Solar Radio Flux Monitors

Characteristics of the systems appearing in this section are provided in Table 7.

2.2.2.2.1 Radio Heliograph, France (System 4A)

This system consists of 47 antennas with sizes in the range 2-10 m, distributed along two arrays in the EW and NS directions. The EW and NS baselines range from roughly 50 to 3 200 m and 2 440 m respectively. The NRH observes the sun between 0830 and 1530 UT daily, at up to ten frequencies between 150 and 450 MHz, with subsecond cadence. It maps the quiet, active, and flaring solar radio emissions. Its observations locate radio sources identified by full-Sun spectrographs and allow one to connect them with signatures of flares and CMEs observed in other spectral ranges. Data are provided the day of the observation for scientific research via the web site http://secchirh.obspm.fr/index.php.

2.2.2.2.2 Radio Solar Telescope Network (RSTN) – Radio Interference Monitoring System (RIMS) (System 4B)

The worldwide RSTN observing system, a part of the Solar Electro-Optical Network (SEON), provides 24 hour a day, 7 day a week monitoring of the Sun. Radio telescopes are located in Learmonth, Australia, San Vito, Italy, and in the United States of America, in Sagamore Hill in Massachusetts, Holloman Air Force Base in New Mexico, and Kaena Point in Hawaii. Also see section 2.2.1.2.7.

The RSTN system has two components: the SRS and the RIMS. The RIMS monitors the frequency range of 245 MHz to 15 400 MHz at eight frequencies. An 8.5 m diameter antenna is used to monitor the lower corona at 245 MHz and the upper chromosphere at 410 MHz and 610 MHz. A 2.4 m diameter antenna is used to monitor the upper chromosphere at 1 415 MHz, the middle chromosphere at 2 695 MHz and 4 995 MHz, and the lower chromosphere at 8 800 MHz. A 0.9 m diameter antenna is used to monitor the lower chromosphere at 15.4 GHz.

2.2.2.2.3 F10.7 cm solar radio flux observations

Microwave emission from the Sun, specifically the F10.7 index (the solar radio flux at 10.7 cm, 2.8 GHz) correlates with solar extreme ultraviolet (EUV) emission on timescales of days and longer and has been measured daily since 1947. This correlation and the transparency of the atmosphere to microwave signals has led to the use of F10.7 as a proxy measurement for solar EUV irradiance, which heats and ionizes the Earth’s atmosphere but cannot be observed from the ground. A range of stations around the world measure integrated solar emissions at the F10.7 cm solar radio flux. Some of these are detailed below – note that these stations typically make observations at other wavelengths than 10.7 cm.

2.2.2.2.3.1 Dominion Radio Astronomy Observatory (DRAO) - System 4C

The National Research Council of Canada has been measuring at 10.7 cm wavelength since February, 1947. Originally sited near Ottawa, Canada it has since moved to the DRAO, Penticton. These observations form the most widely referenced solar radio flux at any frequency. These observations form a baseline of solar activity, historically surpassed only by sunspot numbers. Sunspot numbers were originated in 1848 and have been extrapolated back to around 1750, albeit with gaps in the data.

There is now a multi-wavelength solar flux monitor, measuring fluxes at 21 cm, 18 cm, 10.7 cm, 9.1 cm, 6 cm and 3.6 cm. It is also capable of measuring transient events simultaneously at these wavelengths with millisecond time resolution. The system is currently being evaluated and calibrated. The system uses a specially-designed feed so that “progressive under-illumination” can be used to keep the antenna beam pattern from narrowing with decreasing wavelength. The hardware permits implementation of additional wavelengths between 21 and 3.6 cm.

A similar system is planned for Humain, Belgium **(System 4D)**.

2.2.2.2.3.2 China Solar Radio Telescopes (System 4E)

These systems are deployed in Yunnan, Jiangsu, Shandong, Xinjiang and Beijing. The solar radio telescopes consisting of the antenna subsystem, receiver subsystem, data processing subsystem and monitor subsystem are used to collect, process, restore and transfer the solar radio signal in the 10.7 cm, 6.6 cm and 3.3 cm bands, as in Fig. 14 above. The antenna collects the solar radio emissions including quiet and active status. The analogue receiver amplifies the radio signal and can reject some Radio Frequency Interference through the use of integration analogue filters.

2.2.2.2.3.3 Icheon (System 4F)

The Korean Space Weather Center (KSWC) is Korea’s official source for space weather alerts and warnings. KSWC operates two ionospheric observatories, one in Icheon and one in Jeju. The instruments are complemented by an F10.7 centimetre solar radio flux meter housed in Icheon. All these data are available in real time at http://spaceweather.rra.go.kr.

3 Technical and operational parameters of space weather sensors

Space weather sensors include a wide variety of systems, which may include both transmit and receive or receive only, and may be located on the ground, in the air or on satellites in Earth orbit and beyond. In order to understand how RF-based space weather observing systems fit into the existing radiocommunication services, it is necessary to document the technical and operational characteristics of the observing systems. This listing of systems should not be construed as comprehensive.

TABLE 4

RNSS and other receivers used for space weather observations

Parameter	Unit	System 1A GNSS Ionospheric Scintillation RX	System 1B Chinese GNSS Monitors	System 1C LOFAR	System 1D NENUFAR
Frequency Range of Operation	MHz	GPS L1: 1 565-1 585 MHz, GPS L2P/L2C: 1 217-1 237 MHz, GPS L5: 1 166-1 186 MHz GLONASS L1C/A: 1 597-1 606 MHz GLONASS L2C/A: 1 242-1 249 MHz GLONASS L2P: 1 238-1 253 MHz GALILEO E1: 1 565-1 585 MHz, GALILEO E5: 1 164-1 218 MHz SBAS L1: 1 565-1 585 MHz QZSS L1: 1 565-1 585 MHz, QZSS L2C: 1 217-1 237 MHz, QZSS L5: 1 166-1 186 MHz	1 575.42 1 227.6 1 561.098 1 207.14 1 176.45	10-90; 110-190; 170-230; 210-250	10-85
Maximum receiver antenna gain in upper hemisphere (*x* in the range of *y*)	dBi	6.0	4	45 (10-90 MHz) 73 (110-250 MHz)	39 @ 30 MHz
RF filter 3 dB bandwidth	MHz	Not available	30	80 MHz	80 MHz
Pre-correlation filter 3 dB bandwidth (MHz)	MHz	27 MHz around centre frequency of signal of interest. Cut at 1 610 MHz for GLONASS L1	6 (1M code) 10 (2M code) 24 (10M code)	80 MHz	80 MHz
Receiver system noise figure (*x* in the range of *y*)	dB	2.6	290 (noise temp)	10 (10-90 MHz) 11 (110-190 MHz) 13 (210-250 MHz)	< 22 dB @ 20 MHz < 9 dB @ 80 MHz
Tracking mode threshold power level of aggregate narrow-band interference at the passive antenna output (dBW)	dBW	−80 dBW (for −158 dBW RNSS signal, interference mitigation enabled)	–165	–80	Not Applicable
Acquisition mode threshold power level of aggregate narrow-band interference at the passive antenna output (dBW) (*x* for the bandwidth and integration time of *y*; if given)	dBW	−93 dBW (for −158 dBW RNSS signal, interference mitigation enabled)	–180	–80	−157 @ 20 MHz −130 @ 80 MHz

TABLE 5

Ionospheric sounders and radars

Parameter	Unit	System 2A SuperDARN	System 2B Lowell Ionosonde	System 2C Chinese Ionosonde	System 2D Finnish Ionosonde	System 2E Mexican Ionosonde	System 2F AIS_INGV	System 2G Millstone Hill ISR	System 2H PFISR
Frequency range of operation	MHz	8.0-207	0.5-30.0	1.0-30	0.5-16	1.6-33	1.0-20.0	427-453	449.0-450.0
Transmit power	dBW	140 (peak)	21 (peak) Per each of 2 channels	≤ 30 per channel	7.0	3-20	250 W	Up to 64 dBW	61.0-63.0 Duty Cycle (1-10%)
Signal modulation	Type	Pulse (7 bit pulse code)	Pulse (w/compression −16-chip complementary-coded phase modulation)	Pulse (16-chip complementary-coded phase modulation)	Linear FM	Linear FM	Pulse (w/compression −16-chip complementary-coded phase modulation)	Pulsed with and without phase coding / compression	Pulsed BPSK
Receive sensitivity	dBm	Not available	−130 (11 dB NF)	−112 (10 dB S/N)	Not available	−120 (10 dB S/N)	−85 dBm for 0 dB S/N	Not available	−130
Pulse width	μS	300	533	533	Not available	N/A	480	15 to 2 000 usec	1.0-2 000.0
Pulse spacing	mS	100	5.0 and 10.0	8,532	Not available	N/A	8	3 msec to 40 msec	1.0-25.0
Transmit bandwidth (20 dB unless otherwise specified)	kHz	10.0	42	50	Not available	Not available	60 at 15 dB BW	Not Available	250
Receive RF (3 dB) bandwidth	kHz	1.0 MHz, 50 kHz (switchable)	2 MHz	30 MHz	Not available	15	Variable	25 MHz	5 000
Receive IF (3 dB) bandwidth	kHz	10 kHz (analogue)	30	150 kHz	Not available	0.5, 2.4, 6	66	Varies by signal processing settings and geophysical mode measured	33.0-3 500
TX antenna main beam gain	dBi	23	2.0	5 (at 10 MHz)	Not available	Not available	1 @ 10 MHz	68 meter antenna: ~45 dBi 46 meter antenna: ~42 dBi	43
RX antenna main beam gain	dBi	23	2.0	5 (at 10 MHz)	Not available	Not available	1 @ 10 MHz	See above	43

TABLE 5 (*continued*)

Parameter	**Unit**	**System 2A SuperDARN**	**System 2B Lowell Ionosonde**	**System 2C Chinese Ionosonde**	**System 2D Finnish Ionosonde**	**System 2E Mexican Ionosonde**	**System 2F AIS_INGV**	**System 2G Millstone Hill ISR**	**System 2H PFISR**
TX antenna main beam width (horizontal)	Degrees	4.0 at 10 MHz 3.0 at 14 MHz 2.0 at 18 MHz	−30	30 (at 10 MHz)	Not available	Not available	30 (3 dB @ 10 MHz)	68 meter antenna: ~0.75 deg FWHM 46 meter: ~1.2 deg FWHM	1.1
RX antenna main beam width (horizontal)	Degrees	Not available	30	120 (at 10 MHz)	Not available	Not available	30 (3 dB @ 10 MHz)	See above	1.1
TX antenna	Type	Array of 16 horizontal twin terminated folded dipoles	Cross delta	Cross delta	Rhombic (vertical)	30 m Dipole	Delta	46 meter parabolic prime focus antennas. 68 meter = fixed in zenith direction, 46 meter = fully steerable.	Phased array of crossed dipoles (Transmits RHCP)
RX antenna	Type	Array of 4 horizontal twin terminated folded dipoles	4 crossed-loops	Cross loop	Rhombic (vertical)	30 m Dipole	Delta	See above	Phased array of crossed dipoles (Receives LHCP)

TABLE 5 (*continued*)

Parameter	Unit	System 2I RISR-N	System 2J Tromso VHF Radar (EISCAT)	System 2K Tromso UHF Radar (EISCAT)	System 2L Kiruna VHF Radar (EISCAT)	System 2M Sodankyla VHF Radar (EISCAT)	System 2N Longyearbyen UHF Radar (EISCAT)
Frequency range of operation	MHz	440.9-444.9	214.3-234.7 (RX) 222.7-225.4 (TX)	921.0-933.5 (RX) 926.6-930.5 (TX)	224.0-230.5 (RX)	224.0-230.5 (RX)	485.0-515.0 (RX) 498.0-502.0 (TX)
Transmit power	dBW	61.4-63.0 Duty Cycle (6-10%)	1.6 MW (peak) 200 kW (avg)	2.0 MW (peak) 250 kW (avg)	Not applicable	Not applicable	1 MW (peak) 250 kW (avg)
Signal modulation	Type	Pulsed BPSK	Pulsed binary phase coded	Pulsed binary phase coded	Not applicable	Not applicable	Pulsed binary phase coded
Receive noise temperature	K	−130	250-350	90-110	180-200	180-200	65-80
Pulse width	µS	1.0-2 000.0	1-2 000	1-2 000	Not applicable	Not applicable	0.5-2 000
Pulse spacing	mS	1.0-25.0	0-1	0-1	Not applicable	Not applicable	0-1
Transmit bandwidth (20 dB)	kHz	1 000	8 000	8 000	Not applicable	Not applicable	8 000
Receive RF (3 dB) bandwidth	kHz	5 000	20 000	7 500	30 000	30 000	60 000
Receive IF (3 dB) bandwidth	kHz	33.0-3 500	7 500	7 500	7 500	7 500	7 500
TX antenna main beam gain	dBi	43	46	48	Not applicable	Not applicable	42-45 dBi
RX antenna main beam gain	dBi	43	46	48	48	48	42-45 dBi
TX antenna main beam width (horizontal)	Degrees	1.1	0.8	Not available	Not applicable	Not applicable	1.0-1.3
RX antenna main beam width (horizontal)	Degrees	1.1	0.8	Not available	3.1	3.1	1.0-1.3
TX antenna	Type	Phased array of crossed dipoles (transmits RHCP)	Steerable parabolic cylinder	Steerable parabolic reflector	Not applicable	Not applicable	Steerable parabolic reflector and fixed parabolic reflector
RX antenna	Type	Phased array of crossed dipoles (receives LHCP)	Steerable parabolic cylinder	Steerable parabolic reflector	Steerable parabolic reflector	Steerable parabolic reflector	Steerable parabolic reflector and fixed parabolic reflector

TABLE 5 (*end*)

Parameter	**Unit**	**System 2O** **Skibotn Radar** **(EISCAT_3D)**	**System 2P** **Kaiseniemi and Karesuvato Radars (EISCAT_3D)**	**System 2Q** **MAARSY Radar System**	**System 2R** **TomoScand**
Frequency range of operation	MHz	218.28-248.28 (RX) 230.016-236.544 (TX)	218.28-248.28 (RX)	53.5	140 MHz 400 MHz
Transmit power	dBW	5 000 kW (peak) 1 250 kW (avg)	Not Applicable	800 kW (peak)	Not Applicable
Signal modulation	Type	Pulse with amplitude and phase coding	Not applicable	Single pulse, complementary and Barker codes Pulse shapes: square, Gaussian, shaped trapezoid	CW
Receive noise temperature	K	250	200	Not available	85 at 140 MHz, 75 at 400 MHz
Pulse width	µS	0.4-3 000	Not applicable	0.33-200	Not applicable
Pulse spacing	mS	0-0.5	Not applicable	≥ 0.033	Not applicable
Transmit bandwidth (20 dB)	kHz	6 000	Not applicable	4 000	Not applicable
Receive RF (3 dB) bandwidth	kHz	30 000	30 000	Not available	6 000 at 140 MHz 8 000 at 400 MHz
Receive IF (3 dB) bandwidth	kHz	Not applicable	Not applicable	1, 1.5, 3 and 6 MHz	Not applicable
TX antenna main beam gain	dBi	45	Not applicable	33.5	Not applicable
RX antenna main beam gain	dBi	45	45	33.5	7 at 140 MHz 8 at 400 MHz
TX antenna main beam width (horizontal)	degrees	1.0	Not applicable	Not available	Not applicable
RX antenna main beam width (horizontal)	degrees	1.0	1.0	Not available	140 at 140 MHz 120 at 400 MHz
TX antenna	Type	Phased array with approx. 10 000 drooped, crossed-dipole elements	Not applicable	Not available	Not applicable
RX antenna	Type	Phased array with approx. 10 000 drooped, crossed-dipole elements	Phased array with approx. 10 000 drooped, crossed-dipole elements	Not available	Dual-band Quadrifiliar Helix (1st gen), Stepped Trap Turnstile (2nd gen)

TABLE 6

Solar spectrographs

Parameter	Unit	System 3A e-CALLISTO Radio-spectrometer	System 3B Nancay Decameter Array	System 3C ARCAS	System 3D RoK Jeju	System 3E RoK Icheon
Frequency range of operation	MHz	45.0-890.0	10-80	45-450	30-500	30-2 500
Bandwidth	kHz	825 000	80 000	400 000 98 kHz freq. resolution	1 000	10 000
Receive sensitivity	dBm	−110	−140 dBm/Hz	−110	−112 dBm/Hz	−156 dBm/Hz
Receive IF (3 dB) bandwidth	kHz	180, 300, 2 400	39	20 000 the whole band is scanned by “chunks” of 20 MHz overlapping	Not available	Not available
Antenna main beam gain	dBi	6 per single antenna 35 for full array	6 dB (at 25 MHz) for one antenna 25 dB (at 25 MHz) for each RH/LH array	10 @ 50 MHz 12 @ 250 MHz 14 @ 440 MHz	Not available	Not available
Antenna pattern	Type	LWA, Yagi, LPDA Parabolic dish	Main lobe of ~90° for one antenna Main lobe of 6 × 10° for the full array	Steerable Log Periodic antenna	10 m Log-periodic Antennas	6.4 m · 10 m Parabolic Dish, 6 m Log-periodic Antennas

TABLE 6 (*end*)

Parameter	Unit	System 3F ARTEMIS	System 3G Yamagawa	System 3H ORFEES	System 3I	System 3J HSRS
Frequency range of operation	MHz	20-650	70-9 000	140-1 000	232-258, 389-431, 500-18 000	275-1 495
Receive noise figure	dB	3.0	Not available	1.6	1.6, 4.3	< 5 dB
Receive RF (3 dB) bandwidth	kHz	1 000	31.25 kHz (70 to 1 024 MHz) 1 000 kHz (1 024 to 9 000 MHz)	860 000	18 000 000	1 220 000
Receive IF (3 dB) bandwidth	kHz	Not available	Not available	170 000	500 000	20 000 the whole band is scanned by "chunks" of 20 MHz overlapping
Antenna main beam gain	dBi	21	Not Available	5 to 6	13, 9.4-40.5	15-25
Antenna pattern	Type	Steerable parabolic antenna (110 to 650 MHz); Fixed antenna (20 to 110 MHz)	8 m parabola antenna	Parabolic antenna log periodic (5 m)	Yagi, Parabolic	Steerable parabolic antenna with log periodic feed

TABLE 7

Solar flux monitors

Parameter	**Unit**	**System 4A Nancay**					**System 4B RSTN-RIMS**[(1)]							
Frequency range of operation	MHz	150	236	327	410	432	245	410	610	1 415	2 695	4 995	8 800	15 400
Minimum solar flux observed[(2)]	10^{-22} W/m^2-Hz	N/A	10	16	21	22	10	20	35	55	70	110	230	525
Receive RF (3 dB) bandwidth	MHz	0.700	0.700	0.700	0.700	0.700	10	3.9	6	27	100	50	50	50
Antenna main beam gain	dBi	5	5	5	5	5	24.6	29	32.5	28.8	34.4	39.8	44.7	41
Antenna pattern	Type	Not available					8.5 m parabolic	8.5 m parabolic	8.5 m parabolic	2.4 m parabolic	2.4 m parabolic	2.4 m parabolic	2.4 m Parabolic	0.9 m parabolic

(1) Typical bandwidths are presented.

(2) Observed minimum solar radio fluxes are from typical values observed during the minimum of the recorded solar cycles, and daily values may be lower.

TABLE 7 (*continued*)

Parameter	**Unit**	**System 4C DRAO Penticton**							**System 4D Humain (planned)**					
Frequency range of operation	MHz	1 400-1 427	1 660-1 670	2 750-2 850	2 759-2 850	3 250-3 350	4 990-5 000	8 275-8 375	1 400-1 427	1 660-1 670	2 750-2 850	4 990-5 000	8 275-8 375	10 600-10 700
Minimum solar flux observed	10^{-22} W/m^2-Hz	45	50	65	65	68	106	210	45	Not available	65	106	Not available	Not available
Receive sensitivity noise temperature	K dBm	200	200	220	300	220	230	250	Not available	Not available	Not available	Not available	Not available	Not available
Receive RF 3 dB bandwidth	MHz	12 000/ 27	12 000/ 10	12 000/ 100	100	12 000/ 100	12 000/ 10	12 000/ 100	27	10	100	10	100	100
Receive IF 3 dB bandwidth	kHz	No IF							~12 000	~12 000	~12 000	~12 000	Not available	Not available
Antenna main beam gain	(dBi)	35	35	37	36	37	28	37	31	33	37	42	Not available	Not available
Antenna type	Type	Parabolic reflector	Parabolic reflector	Parabolic reflector	Parabolic reflector	Parabolic reflector	Parabolic reflector	Parabolic reflector	Steerable parabolic antenna with horn	Steerable parabolic antenna with horn	Steerable parabolic antenna with horn	Steerable parabolic antenna with horn	Steerable parabolic antenna with horn	Steerable parabolic antenna with horn

TABLE 7 (*end*)

Parameter	**Unit**	**System 4E China**			**System 4F Icheon**	**System 4G Nobeyama**				**System 4H LOFAR**	**System 4I Japan IPS**	**System 4J IPS Mexico**	**System 4K NENUFAR**
Frequency range of operation	MHz	2 801 ±5%	4 541 ±5%	9 084 ±5%	2 800	1 000	2 000	3 750	10-85	10-90; 110-190; 170-230; 210-250	327	139.6	10-85
Minimum solar flux observed	10^{-22} W/m^2-Hz	65	Not available	Not available	65	Not available	Not available	5	3.6	Not available	Not available	Not available	Not available
Receive noise temperature	K	170	170	170	Not available	Not available	Not available	527 K	288 K	395 K (110-190 MHz); 177 K (170-230 MHz); 122 K (210-250 MHz)	60	10 000	~45 000 at 20 MHz ~1800 at 80 MHz
Receive RF 3 dB bandwidth	(MHz)	1.0	1.0	1.0	Not available	10	10	20	20	80 MHz	20	2	80 MHz
Receive IF 3 dB bandwidth	(kHz)	1 000	1 000	1 000	Not available	10 000	10 000	10 000	10 000	80 MHz	10 MHz	Not available	Not available
Antenna main beam gain	(dBi)	38	40	41	31.4	29	31	33	40	45 (10-90 MHz) 73 (110-250 MHz)	45 dB (Tokoyama); 43 dB (Fuji, Kiso)	Not available	39 at 30 MHz
Antenna pattern	Type	Parabolic reflector	Parabolic reflector	Parabolic reflector	Parabolic	Parabolic reflector	Parabolic reflector	Parabolic reflector	Parabolic reflector	Phased-array beam-formed	Single beam	Multi beam	Phased-array beam-formed

TABLE 8

Riometers

Parameter	System 5A	System 5B
Frequency range of operation (MHz)	30-50	Approx. 30, 38.2 and 20 to 100
Receive noise temperature (dB)	4 350°K/mA	740
Receive RF (3 dB) bandwidth (kHz)	0.2515, 30, 100	0.25
Receive IF (3 dB) bandwidth (kHz)	250	Not available
Antenna main beam gain (dBi)	4.3	23
Antenna type	Twin dipole	Not available
Antenna pattern	Vertical (zenith pointed)	Not available

TABLE 9

Other systems

Parameter	AARDDVARK	Scintillation monitor
Frequencies of operation (MHz)	0.013-0.05 MHz, i.e. 13-50 kHz	327
Transmit power (dBW)	Receive signals of opportunity from VLF communications transmitters	Receive only
Signal modulation	MSK	Not applicable
Duty cycle (percentage)	100	Not applicable
Receive noise temperature (K)	N/A	N
Receive noise floor (dBm)	15	−111
Receive RF (3dB) bandwidth (kHz)	50 kHz	10 000
Receive IF (3 dB) bandwidth (kHz)	0.12 kHz	Not available
Receiver input compression level (dBW)	N/A	Not available
Receiver survival level (dBW)	N/A	Not available
Antenna main beam gain (dBi)	N/A	45 dB (Toyokawa), 43 dB (Fuji, Kiso)
Antenna pattern	Omni-directional	Parabolic Cylinder antenna
Antenna beamwidth (degrees)		Elev: 0.6 degree (Toyokawa), 2.6 degree (Fuji), 1.9 degree (Kiso) Az: 1.3 degree (Toyokawa), 0.5 degree (Fuji), 0.7 (degree)
Required signal to noise ratio (dB)	10 dB	Not Available

4 Appropriate radio service designations for space weather sensors

Taking into account the technical and operational characteristics of systems, the radio service that may be applied to the systems identified in § 3 can be evaluated. Several frequency bands in use by space weather instruments are allocated to the RAS and EESS (passive) and can potentially provide space weather some level of regulatory protection to the degree that the particular space weather application falls within the definition of the allocated radio service. However, if the particular space weather application does not fall within the definition of the allocated science service then it is not entitled to claim protection from RFI events that may occur nor can the space weather application operators legitimately report those RFI occurrences to regulatory authorities.

To assist the reader with the material in §§ 4.1 to 4.6, the following radio service definitions are extracted from the Radio Regulations.

Radiodetermination: The determination of the position, velocity and/or other characteristics of an object, or the obtaining of information relating to these parameters, by means of the propagation properties of *radio waves*.

Radiolocation: *Radiodetermination* used for purposes other than those of *radionavigation*.

Radiolocation service: A *radiodetermination service* for the purpose of *radiolocation*

Radio astronomy: Astronomy based on the reception of *radio waves* of cosmic origin.

Radionavigation: *Radiodetermination* used for the purposes of navigation, including obstruction warning.

Radionavigation-satellite service: A *radiodetermination-satellite service* used for the purpose of *radionavigation*.

Meteorological aids service: A *radiocommunication service* used for meteorological, including hydrological, observations and exploration.

4.1 RNSS-based observations

Table 4 contains characteristics of representative space weather sensor systems that rely on the reception of RNSS signals. It should be noted that the term navigation is not defined in the Radio Regulations. Work in the ITU-R working party responsible for RNSS has resulted in the conclusion that the most commonly accepted definitions for navigation include the requirement that the position of an object must be known, and for RNSS remote sensing applications, the position and velocity of the remote sensing system must be known to produce a data product.

4.2 Ionospheric radars and sounders

Table 5 contains the characteristics of representative ionospheric sounders and radars that are operated as space weather sensors.

4.2.1 Ionospheric radars

The radiolocation service would appear to be applicable to radars used for ionospheric measurements relating to space weather detection and prediction (see Table 10).

TABLE 10

Frequencies identified to be in use by ionospheric radars

Frequency (MHz)	Bandwidth (MHz)	Radiolocation allocation status
13.0	8.0	No allocation
6.5	7.0	No allocation
40.8	0.17	No allocation
53.5	Not available	No allocation
233.28	30	Region 1: No allocation: 218.28-248.28 MHz Region 2: No allocation: 218.28-225 MHz Secondary allocation: 225-235 MHz No allocation: 235-248.28 Region 3: No allocation: 218.28-223 MHz Secondary allocation: 223-235 MHz No allocation: 230-248.28 MHz
224.5	20.4	Region 1: No allocation: 214.3-234.7 MHz Region 2: No allocation: 214.3-225 MHz Secondary allocation: 225-234.7 MHz Region 3: No allocation: 214.3-223 MHz Secondary allocation: 223-230 MHz No allocation: 230-234.7 MHz
442.9	4.0	Secondary allocation
449.5	1.0	Secondary allocation
927.25	12.5	Secondary allocation: 921-933.5 MHz

4.2.2 Ionospheric sounders

Ionospheric sounders transmit signals that are reflected by the ionosphere back to a receiver, providing data value in measuring the characteristics of the ionosphere. It is worth noting that, in addition to space weather-related measurements, these systems are used for ionospheric communications planning. Some locations may be operated to provide space weather data as well as data for communications planning. For space weather purposes, the system description implies that they would also fall under the radiolocation service.

Review of system characteristics and operations has revealed that there is no consistency in the frequencies used within the 0.5 to 30 MHz frequency range. In addition, no allocations to the radiolocation service exist in the frequency range of 0.5 to 30 MHz with the exception of multiple allocations limited to the application of oceanographic radars, which are not useful for space weather observations.

4.3 Solar Spectrographs

Table 6 contains the characteristics of solar spectrograph systems. These receive-only systems receive wideband radio emissions from the Sun, in a manner that radio astronomy stations receive radio emissions from celestial bodies. While many frequency ranges used are also used for radio astronomy, solar observations currently do not fall under the definition of the radio astronomy service. Solar spectrograph operations require use of many discrete frequencies over the frequency range of 10 to 300 MHz[2]. The extremely broad range of frequencies required seem to make it impractical to create an allocation to a radio service that is applicable solar spectrographs.

4.4 Solar Flux Monitors

Table 7 contains the characteristics of solar flux monitors. These receive-only systems receive radio emissions from the Sun, in a manner similar to how radio astronomy stations receive radio emissions from celestial bodies. While some frequency ranges used are also allocated to radio astronomy, solar observations currently do not fall under the definition of the radio astronomy service (see Table 11).

TABLE 11

Frequencies identified to be in use by Solar Flux Monitors

Frequency (MHz)	Radio astronomy allocation status
150	No allocation
236	No allocation
245	No allocation
327	Primary allocation (322-328.6 MHz)
410	Primary allocation (406.1-410 MHz)
435	No allocation
610	No allocation
1 200	No allocation
1 415	Primary allocation (1 400-1 427 MHz)
1 665	Primary allocation (1 660.5-1 668 MHz)
2 695	Primary allocation (2 690-2 700 MHz)
2 800	No allocation
3 750	No allocation
4 541	No allocation
4 995	Primary allocation (4 990-5 000 MHz)
8 325	No allocation
8 800	No allocation
9 084	No allocation
9 400	No allocation
10 650	Primary allocation (10 600-10 680 MHz)
15 400	Primary allocation (15 350-15 400 MHz)

[2] One system has been identified as extending operations up to 18 000 MHz, but this system appears to be significant outlier from typical operations.

4.5 Riometers

Table 8 contains the characteristics of representative riometer systems. Riometers are receive-only systems that measure the opacity of the ionosphere to radio emissions from celestial bodies. The operations are similar to radio astronomy, but the reception of signals from celestial bodies is used to measure the characteristics of the ionosphere and atmosphere of Earth. Therefore, riometer operations may not fall under the definition of radio astronomy. The spectrum requirements for riometer operations that have been identified are fairly generic, covering the large frequency range of 20 to 100 MHz. It is worth noting that no primary allocations to the radio astronomy service exist between 20 and 100 MHz except for the frequency band 73.0-74.6 MHz, in Region 2 only. In addition, secondary allocation exists in the frequency range 37.5-38.35 MHz.

4.6 Other systems

Table 9 provides characteristics of space weather sensor systems that do not fall under any of the previous categories.

4.6.1 AARDDVARK

The AARRDVARK system is a network of receive only stations that receive terrestrial VLF signals of opportunity. The VLF signals may be transmitted by stations operating in the time standard and frequency signal, radionavigation, broadcast, fixed or mobile services. However, since the AARRDVARK receivers receive the signals of opportunity the radio service of the transmit station may not apply to the AARRDVARK receive station. AARDDVARK receives signals at frequencies between 15 and 50 kHz. The following allocations exist within the frequency range, but may not be applicable:

13 to 14 kHz:	Radionavigation
14 to 19.95 kHz:	Fixed, Maritime Mobile
19.95 to 20.05 kHz:	Time Standard and Frequency Signal
20.05 to 50 kHz:	Fixed, Maritime Mobile.

The most applicable service for this application may be the meteorological aids (metaids) service since it is similar to the receive-only metaids operations operating the frequency band 9.0-11.3 kHz. However, no allocation to the metaids service exists in the frequency range of interest.

4.6.2 Scintillation monitors

Table 9 contains the characteristics of a representative scintillation monitor system. Scintillation monitors are receive-only systems that measure the solar winds by receiving radio signals from compact radio sources. The operations are similar to radio astronomy, but the reception of signals from compact radio sources is used to measure the characteristics of the solar winds. Therefore, scintillation monitor operations may not fall under the definition of radio astronomy. One frequency, 327 MHz, has been identified for use by scintillation monitors. It is worth noting that a primary radio astronomy allocation does exist in the frequency band 322-328.6 MHz.

5 Regulatory aspects

This ITU-R Report documents a broad range of space weather sensor systems using radio spectrum that are operated globally. The systems can be categorized (see Annex 1) as those that are 1) used for operational detection, predictions and warnings; 2) under development and may transition to operational use sometime in the future; and 3) those used for research purposes only. Combined, they form a formidable list of systems to address under a single WRC agenda item effort. It is also shown that with some types of systems frequency use around the globe is not consistent, though the systems are limited in number.

While all systems can be afforded some level of regulatory recognition and protection, addressing the systems used for operational detection, prediction and warnings (Category 1) are most critical since they are key to protection of large sectors of national economies and support public safety. In addition, the vulnerability of the receive-only systems are in most need of attention for a regulatory perspective.

Annex 1

Categorization of the RF-based sensors in regards to support of current space weather products

The material contained in the preliminary draft new Report on space weather sensors shows that there is a wide range of systems and frequency bands. The following non-exhaustive categorization of space weather sensor systems using radio spectrum is based on current space weather products reliance on space weather sensor operation as described below.

Category descriptions

1 = Used in operational space weather applications (for real time monitoring, near real time initialisation of forecast models, near real time verification of forecast results, with reliability of near real time data reception > selected threshold)

2 = In process of transition from research to operational use

3 = Research systems currently not used operationally (e.g. data not available in near real time, gaps in data provision).

The following information include a brief summary of space weather radio frequency instruments and their categorization.

TABLE 12

Category 1: Operationally used space weather applications

Instrument/System	Frequency (MHz)	Bandwidth	Location (country/region)	Applicable section in Report
ARCAS and HSRS spectrograph	45-450	400 MHz (98 kHz freq. resolution)	Belgium	2.2.1.2.3
	275-1 495	1 220 MHz		
CALLISTO spectrograph network	45.0-870.0	(MHz) 0.18, 0.30, 2.40	Global	2.2.1.1
RNSS ionospheric monitoring	See Report Table 4: System 1A, 1B		Global	2.1.1, 2.1.1.1, 2.1.1.1.2, 2.1.1.1.3

TABLE 12 (*end*)

Instrument/System	**Frequency (MHz)**	**Bandwidth**	**Location (country/region)**	**Applicable section in Report**
Ionosonde	0.5-30.0	42 kHz	Global	2.1.3.1, 2.1.3.2, 2.1.3.3, 2.1.3.4, 2.1.3.5
	1.0-30	50 kHz		
	0.5-16	Varies		
	1.6-33	Varies		
	1.0-20.0	60 kHz		
Ionosphere D-Region absorption (riometers)	20.5, 30, 38.2, 51.4	(kHz) 0.2515, 30, 100 and ~20 MHz	Canada, Iceland, Argentina, Australia, USA, South Africa, Northern Europe, Greenland, China, Antarctica, Russian Federation, Brazil	2.1.2.1
Ionospheric tomography receivers	140	6.0 MHz	Northern Europe	2.1.8.1
	400	8.0 MHz		
ORFEES Spectrograph	140-1 000	860 MHz	France	2.2.1.2.7
Solar Radio Flux (RIMS)	245, 410, 610, 1 415, 2 695, 4 995, 8 800, 15 400	Varies	Australia, Italy, USA	2.2.2.2.2
Solar Radio Flux (IPS)	327	10 MHz	Japan	2.2.2.1.2
Solar Radio Flux (IPS)	10-90; 110-190; 170-230; 210-250	80 MHz	Europe (LOFAR)	2.2.2.1.1
Solar Radio Flux (IPS)	139.6	Not Available	Mexico	2.2.2.1.3
Solar Radio Flux Monitoring (F10.7)	2 800 MHz	Varies	Canada, Belgium, Japan, China, Korea	2.2.2.4.1, 2.2.2.4.2, 2.2.2.4.3
Solar Radio Spectrograph	Varies	Varies	Global	2.2.1.2.2, 2.2.1.2.4, 2.2.1.2.6, 2.2.1.2.7 and others (not shown)

TABLE 13

Category 2: Systems in transition from research to operational use

Instrument/System	**Location (country/region)**	**Applicable section in Report**
AARDDVARK network of VLF receivers	Global	2.1.9
HF Coherent radar (SuperDARN)	High Latitudes	2.1.5.1
Incoherent Scatter Radar (ISR)	Northern Europe, North America, Japan	2.1.4.1 to 2.1.4.7

TABLE 13 (*end*)

Instrument/System	Location (country/region)	Applicable section in Report
Meteor Radar	Worldwide	2.1.6.2
Radio Heliograph	France	2.2.2.2.1
Solar Radio Flux (IPS)	India, Russian Federation Korea, Finland, Australia	None
Subiono propagation	Japan	None
NENUFAR	France	2.1.2.2.3 and 2.2.2.1.4

TABLE 14

Category 3: Research systems

Instrument/System	Location (country/region)	Applicable section in Report
Decameter array (incl. HF spectrograph)	France	2.2.1.2.1
Ionospheric D-Region absorption of cosmic radio noise (spectral approach)	Finland, Sweden, Norway	None
Ionospheric heaters	Norway (Tromso), USA (Alaska, Puerto Rico), Russian Fed. (Vasilsurks)	2.1.7
HF radio spectrograph	Japan	None
MST radar	USA, India, UK China	None
MLT dynamics radar	Norway, Antarctica, Indonesia, Australia, China	2.1.6.4.1
Radiometer for mesospheric ozone detection	South Africa, Antarctica	None
Spectropolarimeter	Russian Federation	None
Solar radio spectrograph (ARTEMIS)	Greece	2.2.1.2.5
Solar radio imager	Finland, Japan, USA, Russian Federation, India	None
Solar radio telescope	China, Russian Federation	None
Spectrograph	India, Russian Federation, Ukraine, Czech Republic, Switzerland	None